Cell and Tissue Engineering

AIMS Cell and Tissue Engineering, 2(3): 119–162.
DOI: 10.3934/celltissue.2018.3.119
Received: 14 May 2018
Accepted: 13 August 2018
Published: 28 August 2018

http://www.aimspress.com/journal/CTE

*Review*

# 3D bioprinting of the kidney—hype or hope?

**Sanna Turunen[1,2], Susanna Kaisto[3], Ilya Skovorodkin[3], Vladimir Mironov[4,5], Tomi Kalpio[1], Seppo Vainio[3,6] and Aleksandra Rak-Raszewska[3,*]**

[1] 3DTech Oy, Hyvoninkatu 1, 24240 Salo, Finland
[2] Biomaterials and Tissue Engineering Group, BioMediTech and Faculty of Biomedical Sciences and Engineering, Tampere University of Technology, Korkeakoulunkatu 3, 33720 Tampere, Finland
[3] Biocenter Oulu, Faculty of Biochemistry and Molecular Medicine, University of Oulu, Aapistie 5, 90220 Oulu, Finland
[4] 3D Bioprinting Solutions, 68/2 Kashirskoe highway, 115409 Moscow, Russia
[5] Institute for Regenerative Medicine, Sechenov Medical University, Trubetzkaya Street 7, 119991, Moscow, Russia
[6] Faculty of Biochemistry and Molecular Medicine, Biocenter Oulu, InfoTech Oulu, Oulu University and Biobank Borealis of Northern Finland, Oulu University Hospital, 90220 Oulu, Finland

* **Correspondence:** Email: Aleksandra.Rak-Raszewska@oulu.fi; Tel: +359 (0) 469516408.

**Abstract:** Three-dimensional (3D) bioprinting is an evolving technique that is expected to revolutionize the field of regenerative medicine. Since the organ donation does not meet the demands for transplantable organs, it is important to think of another solution, which may and most likely will be provided by the technology of 3D bioprinting. However, even smaller parts of the printed renal tissue may be of help, e.g. in developing better drugs. Some simple tissues such as cartilage have been printed with success, but a lot of work is still required to successfully 3D bioprint complex organs such as the kidneys. However, few obstacles still persist such as the vascularization and the size of the printed organ. Nevertheless, many pieces of the puzzle are already available and it is just a matter of time to connect them together and 3D bioprint the kidneys. The 3D bioprinting technology provides the precision and fast speed required for generating organs. In this review, we describe the recent developments in the field of developmental biology concerning the kidneys; characterize the bioinks available for printing and suitable for kidney printing; present the existing printers and

possible printing strategies. Moreover, we identify the most difficult challenges in printing of the kidneys and propose a solution, which may lead to successful bioprinting of the kidney.

**Keywords:** organ biofabrication; bioprinting of kidneys; organoids; bioink; 3D bioprinters; printing strategy

**Abbreviations:** ADPKD: autosomal dominant polycystic kidney disease; AKI: acute kidney injury; CAD: computer-aided design; CIJ: continuous inkjet; CKD: chronic kidney disease; CT: computed tomography; DBB: droplet-based bioprinting; dECM: decellularized extracellular matrix; DOPsL: dynamic optical projection stereolithography; DOD: drop-on-demand; EBB: extrusion-based bioprinting; ECM: extracellular matrix; ESRD: end stage renal disease; FDA: Food and Drug Administration; FDM: fused-deposition modeling; HA: hyaluronic acid; hiPSCs: human induced pluripotent stem cells; hPSCs: human pluripotent stem cells; HUVECs: human umbilical vein endothelial cells; ITOP: Integrated Tissue-Organ Printer; LBB: laser-based bioprinting; LIFT: laser-induced forward transfer; IR: infrared; LGDW: laser-guidance direct writing; MAPLE-DW: matrix-assisted pulsed laser evaporation-direct write; MAPLE: matrix-assisted pulsed-laser evaporation; MDCK: Madin-Darby canine kidney; MM: metanephric mesenchyme; MRI: magnetic resonance imaging; NPCs: nephron progenitor cells; PAAm: polyacryl amide; PCL: poly(ε-caprolactone); PEG: polyethylene glycol; PEGda: poly(ethylene glycol) diacrylate; PKD: polycystic kidney disease; PLCL: poly(L-lactide-co-caprolactone); qPCR: quantitative polymerase chain reaction; RGD: arginylglycylaspartic acid; RPTECs: renal proximal tubule epithelial cells; SCID: severe combined immunodeficiency; SLA: stereolithography; SMCs: smooth muscle cells; UB: ureteric bud; UBPCs: ureteric bud progenitor cells; UCs: urothelial cells; VEGF: vascular endothelial growth factor; UV: ultraviolet; 2PP: two-photon polymerization

## 1. Introduction

Every year, and only in Europe, 86,000 patients are added to the waiting lists for organ transplantations and majority of them (81%) need kidney transplants [1]. Kidney disease can be either acute or chronic, the latter progressively worsening over time to become an end stage renal disease (ESRD)—a stage when kidneys are non-functional. At the present, the only treatment options for ESRD are transplantation or dialysis, both of which have severe drawbacks in terms of morbidity, mortality and the economic costs [2]. Moreover, the incidence of ESRD is rising annually, with more than 3000 people added monthly to the transplantation waiting list, and therefore alternative therapies are needed. Most people have two kidneys and even though it is possible to live with one kidney, living donations are very rare while the organs from deceased donors do not meet the existing demand for organs. Hence, a new approach to obtain organs for transplantations is needed, and we see a great opportunity in three-dimensional (3D) bioprinting technology to provide those desperately needed organs.

Organ biofabrication has significant potential. The 3D printing allows the generation of precise,

customized, and complex structures, and it is expected to revolutionize the field of regenerative medicine. The automation of bioprinting enables the creation of customized structures that can be printed with extraordinary precision [3]. 3D printed plastic models of complex tumors, bone fractures or other trauma, generated on the basis of images gained from computed tomography (CT) or magnetic resonance imaging (MRI), have already been used in medicine to educate doctors and to provide an excellent and super precise training platform before operating on the patient's tissues [4]. However, bioprinted tissues present another level of difficulty, namely living cells. Some simple tissues such as cartilage have already been printed with success [5]. However, the bioprinting of soft tissues or complex organs, such as the kidneys, will require careful development and selection of the "printing ink"—the combination of cellular material and biomaterials that support cell survival and growth [6,7]. Nevertheless, some progress has already been made and recently 3D bioprinting of a functional thyroid gland has been reported [8].

Kidneys are important organs that play vital roles in removing waste products from organisms and their development has been studied for the last six decades [9]. Kidney development begins at embryonic day (E) 10.5 when the ureteric bud (UB) grows from the Wolffian duct towards the metanephric mesenchyme (MM). Once the UB invades the MM, it divides dichotomously and induces MM to condense around the UB tips. This first contact starts the molecular crosstalk between these two tissues where various genes and signaling pathways are activated. The MM cells form condensates known as the cap MM, which undergo polarization and epithelialization processes, leading to the formation of renal vesicles, which develop into Comma- and then S-shaped bodies. The latter elongates and forms nephrons with glomeruli at the apical site, while the distal site connects with the UB. During this process called nephrogenesis, the MM gives rise to the basic functional kidney unit, the nephron, and the UB gives rise to the collecting duct system [10–12]. Well-developed nephrons filter blood and generate urine, which drains into the calyces and via the ureter into the bladder where the process of micturition leads to its removal from the organism.

Kidneys are complex organs build from many different cell types composing those of kidney and vasculature, and even though adult stem cells have been found in many organs [13], in kidneys their capacity to regenerate an organ is very limited. On the other hand, embryonic kidneys have the remarkable capacity to self-assemble and generate rather well-segmented nephrons [14–16] giving rise to embryonic kidney rudiments during a reaggregation process. Specifically, the dissociated kidney cells can form renal organoids, cell aggregates that contain more than one type of renal cells [17,18]. These organoids become vascularized upon transplantation under the kidney capsule of nephrectomized athymic rats [19], and generate glomeruli with functional podocytes [20]. Similar results have been obtained when renal organoids were transplanted subcutaneously [21].

In this review, we broadly present all main features and requirements for 3D bioprinting of the kidneys, and optimistically look into the future, where 3D bioprinting is no longer a hype but hope for many kidney patients.

## 2. Cellular component

When considering 3D bioprinting of the tissue, one needs to know the organ of interest thoroughly as the living cells are one of the main components of bioprinting. Nephron is the

structural and functional unit of the kidney and it is composed of nine main parts, such as the glomeruli, the convoluted proximal tubule, the straight proximal tubule, the descending limb of the loop of Henle, the thin ascending limb of the loop of Henle, the thick ascending limb of the loop of Henle, the straight distal tubule, the macula densa, and the convoluted distal tubule. The latter connects to the collecting duct, which also builds up few levels of the kidney structures, such as the renal pyramids, the minor calyces, the major calyces, the renal pelvis and the ureter. Each of these parts is structurally different and contains at least three types of cells, each playing a significant and very specific role during the urine production process. However, not only the great variety of cells makes the organ complex, but also the number of nephrons, which per kidney, on average is one million [22]. When we add the vascular network starting from the glomerular capillaries via the peritubular capillaries ending at the vase rectae [23], the complexity of the organ increases dramatically.

### *2.1. Printing with single cells*

The vast variety of cells constituting the many nephrons of the kidney and the size of the organ has proven to be challenging for 3D bioprinting. 3D bioprinting of the kidney using a single-cell technique would require the differentiation and culture of many different functional cell types *in vitro*. Moreover, it would require a very detailed 3D map of the kidney with all different cell types appropriately positioned and a 3D bioprinter with several printing nozzles to enable an exact positioning of each cell. With this process, even though automatized, it would take a very long time to print an organ, not to mention the diversity of cells that need to be cultured beforehand. However, currently the variety of human renal cells in culture (i.e. the cell lines) are limited to proximal tubules [24] and podocytes [25], which is only a fraction of what would be needed for a fully functional kidney.

### *2.2. Printing with organoids*

However, the nature provides an excellent alternative to the use of single cells. Dissociated and re-aggregated embryonic kidneys are able to generate compact renal organoids, which contain functional nephrons [15,16,26] with most of the required cell types present. Moreover, these organoids in the form of spheres or clusters of cells represent several cell types typical of the organ they mimic [17,18], in the case of the kidney nephrons or nephrons and collecting ducts. The organoids follow the developmental process of the kidney development. Namely, first the pre-tubular aggregate is formed, giving rise to the renal vesicle. Cells in the renal vesicle polarize and lay down the basement membrane generating the Comma-shape body and the S-shaped body; the latter elongates giving rise to the nephrons with the filtering unit—the glomerulus developing on the proximal end and the distal end connecting to the collecting duct. However, in these organoids, the collecting duct does not form a single compact system, but many disperse ones, therefore presenting lack of drainage.

Recently, big progress has been achieved in generating functional organoids from human pluripotent stem cells (hPSCs) and human induced pluripotent stem cells (hiPSCs). The latter cells present an attractive source for developing cell therapies or generating bioengineered kidney

structures. They can be derived from a specific patient and therefore present lack of graft rejection risk when injected back to the recipient patient. Various methods of hPSC/hiPSC differentiation towards renal progenitors have been proposed and include differentiation in 2D or 3D settings or mix of both, using application of various concentrations of growth factors (see Table 1). These protocols (see Table 1) try to mimic the natural processes occurring during the renal development by inducing the hPSCs/hiPSCs to differentiate through a few stages; first into a primitive streak, then into an intermediate mesoderm and finally into nephron progenitor cells (NPCs). Although the NPCs have been obtained with variable efficiency (10–92%), most of them generated organoids with several nephron specific parts, although their maturity varied greatly [21,27–34]. Organoids generated in the studies by Morizane [33,34] and Takasato [31] presented the best maturity and structurally resembled the kidney orientation. Nephrons formed in these organoids presented a glomerular tuft-like structure (nephrin and podocalyxin$^{+}$) connecting with the proximal tubules (LTL$^{+}$), which connected with the distal tubule (cadherin$^{+}$), which in the case of Takasato protocol, was also connected with the ureter structures; some also presented the markers of the loop of Henle (qPCR data) [31].

Most of these protocols (Table 1) studied the potential of formation of organoids and their functionality *in vitro* showing susceptibility to nephrotoxic agents such as cisplatin or gentamycin [31–33]. The study about a mouse model of acute kidney injury (AKI) induced by ischemia/reperfusion injury showed a therapeutic effect of injected hPSCs-NPCs under the kidney capsule [30] while the subcutaneous injection of hPSCs-NPCs into SCID mice presented partial maturation of glomerular structures and lack of teratoma formation [21]. However, small pieces of the developing cartilage (which, similarly to the kidney, develops from mesoderm) were observed next to the developing nephrons [21].

While the differentiation of hPSCs/hiPSCs into NPCs and their ability to form fully structured and functional nephrons is quite seriously tested in organoids, the differentiation of hPSCs/hiPSCs into ureteric bud progenitor cells (UBPCs) is not so popular. However, a protocol specifically differentiating hPSCs/hiPSCs into the UB progenitor cells has been published (see Table 1) and it derived UB cells that were able to generate chimeric UB structures and induced the nephrogenesis in the MM [35].

The above-mentioned studies show that the generation of renal specific, functional organoids is possible; that they actually have nephron organization and even are capable of mimicking the kidney structure at some level. Hence, in the near future it might be possible to generate organoids containing hPSCs/hiPSCs differentiated towards NPCs and UBPCs and therefore complete, functional human organoids. Therefore, they might be the most feasible source of cells/tissue for the purpose of 3D bioprinting. Researchers have already used spheroids generated from mouse thyroid gland cells and 3D bioprinted functional mouse thyroid gland [8]. Similar technology could also be considered when trying to 3D bioprint the kidneys by using renal organoids.

## 3. Bioink materials for kidney bioprinting

For bioprinting, the choice of the bioink material, i.e. the encapsulating material for cells, is crucial, as it should mimic the complexity of the native ECM while having suitable physicochemical properties for the printing process (printability). The printability refers to several material properties

contributing to the effectiveness and accuracy of the printing process. Most importantly, the viscosity of the bioink needs to be adjustable by either changing the temperature or via shear thinning, for the bioink to be suitable for printing with different printing methods, for example to be dispensed out of the print head nozzles. Secondly, the bioink should be in liquid form before printing to avoid nozzle clogging, but it should also gel either by physical or covalent crosslinking fast after printing to ensure structural integrity of the printed shape. In addition, it would be desirable that the bioink would have a wide biofabrication window, which would allow the adjustment of the material concentration and crosslinking density according to the application in question while still keeping good printing fidelity [36,37].

Besides the perquisite for being easily printable, the bioink has to be biocompatible and biodegradable over long-term *in vivo* implantation in order to facilitate cell attachment, proliferation and differentiation, as well as being resorbed and replaced with natural ECM at a desired rate [37,38]. Optimal bioink should also minimize stress-induced damage to cells and biological components during printing process involving localized heating or pressure-induced extrusion by exhibiting low thermal conductivity or shear-thinning properties [39]. It is also desirable that the bioink material would be commercially available and affordable. In addition, it would be beneficial that the biomaterial is already approved by the Food and Drug Administration (FDA) for use in medical device applications as biocompatibility testing required for obtaining the regulatory approval can be expensive and time-consuming [40].

For soft tissue engineering, such as bioprinting of kidneys, hydrogels are the preferable materials as they can mimic the elastic moduli represented in the soft tissues in the body [41]. Hydrogels are hydrophilic water-insoluble networks of crosslinked polymers capable of absorbing more than 99% water in their network [37,42]. They can be based on either natural (such as collagen, alginate, gelatin, chitosan and hyaluronic acid) or synthetic polymers (such as polyethylene glycol (PEG) and Pluronic® F127). Natural polymers have the advantage of having inherent bioactivity and similarity to the human ECM, but their downsides are weak mechanical properties and lack of control in composition and molecular weight. Synthetic polymers are advantageous bioinks due to their controllable and reproducible chemical structure and physical properties, which allows them to be tailored to suit particular application [43].

Moreover, the decellularized extracellular matrix (dECM) from the kidney contains a variety of proteins, proteoglycans and glycoproteins. It can be isolated from tissue by the removal of all the cells leaving behind the native ECM scaffold [44]. Although decellularization itself is not a new fabrication method, it has only recently been harnessed into producing a new class of hydrogels for 3D bioprinting. These printable tissue-specific dECM bioinks provide a native tissue-like microenvironment for the cells and are thus much more biofunctional than hydrogels composed of only a single component [45–47]. The biggest downside of dECM bioinks is their low viscosity and thus insufficient mechanical stability, which worsens the printing resolution and shape fidelity [39]. As the bioprinting of kidney structures is still in its infancy, not many bioink materials have yet been tested for this application. Thus, we represent here also hydrogel materials that have been tested for 3D renal cell culture purposes, such as culturing proximal tubule epithelial cells, and thus can be potentially used as bioinks for bioprinting of kidney structures. The overview of the characteristics and properties of each of the evaluated hydrogels is collated in Table 2.

### *3.1. Synthetic hydrogels*

Synthetic polymers, such as polyethylene glycol (PEG) and Pluronic® F127, are water-soluble polymers that have been widely used as sacrificial materials (as fugitive ink or support material) for bioprinting complex 3D structures [48,59]. PEG is biocompatible with reduced immunogenicity and approved by the FDA for use in regenerative medicine [60]. However, PEG does not generate hydrogel on its own; instead, it has to be chemically modified if used as bioink. PEG also lacks inherent cell-binding sequences, such as RGD motif, and it is not biodegradable. Thus, to improve their cell compatibility, PEG hydrogels have to be functionalized with cell-binding peptide sequences and enzymatically degradable groups [61]. One of the most used approaches to achieve PEG hydrogel is acrylation. Acrylated PEG (PEGda) can be crosslinked into hydrogel by photoinitiator-mediated photopolymerization using UV-light [62]. However, the photoinitiator should be selected with care, as it will have to be biocompatible, soluble in water, stable and noncytotoxic [63]. Even the most widely used Irgacure photoinitiators are detrimental to cells at concentration exceeding 0.5% (w/v) unless the excess initiator is leached out from the printed structures [64]. PEGda can be used as bioink in all types of printer modalities, including extrusion-based [65], droplet-based [66], and laser-based bioprinting [67].

Polyacryl amide (PAAm) is a synthetic, nonresorbable polymer widely used in ophthalmic operations, drug treatment, and food packaging products [49,68]. PAAm has been clinically proven as a nontoxic and non-immunogenic material and it has the FDA approval. It is hydrophilic in nature and shows good mechanical stability [69]. Other advantages of PAAm include high rate of swelling, high surface area and fast precipitation polymerization reaction leading to almost complete conversion degree [70]. However, the residues of acrylamide monomer have been implicated as potentially neurotoxic, genotoxic, reproductively toxic and carcinogenic, and therefore residual acrylamide monomers must be detected and carefully purified before PAAm can be used as a scaffold [68,71].

Pluronic® F127 is a trade name for synthetic tri-block copolymer composed of a central hydrophobic sequence of poly(propylene glycol) flanked by two hydrophilic chains of poly(ethylene glycol) (PEG). It has been approved by the FDA due to its enhancement of protein stability, lack of myotoxicity, and excellent biocompatibility. Pluronic® F127 is used as a drug delivery carrier and as an injectable gel for the treatment of burns and wounds [72]. It is a thermo-sensitive hydrogel exhibiting solution-gelation transition in an aqueous solution at 15 to 35°C depending on the concentration. The solution-gel transition temperature increases when the Pluronic® F127 concentration decreases [73]. Pluronic® F127 has great potential as a bioink for the extrusion-based bioprinting process but it requires a thermally controlled nozzle system to heat the material above 20°C, where it changes from liquid to viscous and exhibits shear-thinning behavior. In addition, a heated plate to maintain the temperature of the printed structure and to prevent it from melting and losing its shape is also beneficial [59]. Despite its many good properties, Pluronic® F127 is mechanically very weak and degrades in few hours limiting its use as such. Thus, it should be chemically modified by blending with other polymers to improve its mechanical strength. Alternatively, it can be used as a fugitive ink in complex structures as it can be dissolved away at 4°C after printing. This yields to perfusable channels within the bulky constructs [50,74]. Due to its thermosensitive nature and its high viscosity, Pluronic® F127 has not been used as bioink for

droplet-based bioprinting. It is also incompatible with laser-based bioprinting, as it is not viscoelastic and cannot transfer thermal energy to kinetic energy, which is a prerequisite for jet formation [75].

### *3.2. Natural hydrogels*

Natural polymer, the gelatin, is a fibrous protein that is obtained by partial hydrolysis of the triple helix structure of collagen into single-strain molecules [76]. Gelatin is a thermally reversible hydrogel being solid below 37°C and liquefying under physical conditions. It is biocompatible, non-immunogenic and completely biodegradable [77]. However, gelatin is rarely bioprinted in its native form due to its poor mechanical properties, instead it is either chemically crosslinked with crosslinking agents, such as glutaraldehyde, or used as a blend with other hydrogels, such as fibrin [75,78]. Gelatin is not a popular bioink for droplet-based bioprinting, but it has been successfully used for laser-based bioprinting due to its viscoelastic properties and stability [75].

Fibrinogen is a plasma glycoprotein, which in the presence of thrombin and $Ca^{2+}$ assembles into stable fibrous insoluble fibrin gel [79]. It supports extensive cell growth and proliferation, and plays major role in wound healing [80]. The drawback in using fibrin for *in vivo* tissue engineering is its ability to induce severe immune reaction or transfer infectious diseases. However, this can be avoided by producing autologous fibrin from the patient's own blood or by producing fibrin as recombinant protein by mammalian cells [81]. The practical use of fibrin is limited due to its lack of structural integrity and rapid degradation. The non-shear-thinning nature of fibrinogen and thrombin as well as the weak mechanical properties of precrosslinked fibrin makes the extrusion of fibrin challenging. However, droplet-based printing of the two components is a good option, although fibrin's prolonged crosslinking time makes it difficult to print it into desired shape. Due to fibrin's delicate structure, it is not suitable bioink for laser-based bioprinting [75]. The printability of the bioink and the mechanical properties of the printed structure can be improved by using the combination of gelatin and fibrin (or fibrinogen). By this approach, a biocompatible and a stable hydrogel blend for bioprinting can be developed. This blend is crosslinked by dual-enzymatic strategy involving thrombin and transglutaminase upon printing by diffusion of these enzymes from the surrounding matrix. Thrombin is used to rapidly polymerize fibrinogen, whereas transglutaminase being a slow-acting $Ca^{2+}$-dependent crosslinker is needed for long-term mechanical and thermal stability [50,78]. In addition, the elastic modulus of the bioink (~3.5 kPa) mimics nicely the modulus of the cortex of a healthy kidney (~4 kPa), which together with the suitable ECM-like composition is important for the retention of tissue specific cell functionality [50].

Matrigel™ is an ECM protein mixture derived from mouse sarcoma cells and it consists of collagen IV, laminin, perlecan and growth factors, which are also found in the basement membrane of normal tissues. The gelation of Matrigel™ is thermally reversible; it gels at 24–37°C in 30 min. It promotes the differentiation of various cell types as well as vascularization [51]. As an animal product, the disadvantages associated with Matrigel™ is the batch-to-batch variability and possible occurrence of growth factors. Although being a mixture of ECM proteins, Matrigel™ does not reflect the organotypic ECM of kidney, nor is it suitable for transplantation experiments [18]. For extrusion-based bioprinting, Matrigel™ requires a cooling chamber as it needs to be printed before being fully crosslinked. Also, a heating plate is essential, to speed up the crosslinking after printing

and ensure shape maintenance. Matrigel™ has not been used as bioink for droplet-based bioprinting, but it has been used as a substrate for printed cells. However, due to its thermal crosslinking properties and optimal viscosity Matrigel™ is a feasible bioink for laser-based bioprinting. Unfortunately, it is an expensive material, which can limit its use as a bioink [75].

Collagen type I fibril is triple helical protein that is the most abundant ECM molecule in the body. It is widely used in tissue engineering as a growth substrate for 3D cell culture or as a scaffold material for cellular therapies [52,82]. Collagen is highly conserved protein form species to species causing minimal immunological reactions. The collagen matrix stimulates cell adhesion and growth due to the presence of cell-binding RGD sequences in its backbone [75]. The fibril precursors of collagen are acid-soluble and crosslink when the pH, temperature and ionic strength are adjusted near physiological levels. After neutralization at a pH from 7.0 to 7.4, collagen polymerizes within 30–60 min at 37°C [83]. The slow gelation process makes bioprinting of 3D constructs from collagen challenging as the deposited material remains liquid for over 10 min. The poor mechanical properties and the slow gelation rate as well as the instability of collagen due to fast degradation may require the use of supportive hydrogels for collagen structures. The mechanism of collagen crosslinking is suitable for extrusion-based bioprinting, where the printing is started as soon as the collagen begins to polymerize and extruded collagen is incubated until fully crosslinked [59]. Due to collagen's fibrous microarchitecture, its use as a bioink for droplet-based bioprinting is very limited. Instead, due to collagen's sticky nature it can be easily transferred using laser source enabling laser-based bioprinting [75] or extrusion printers as it was used to 3D bioprint the thyroid gland by the 3D Bioprinting Solutions Company using their Fabion 3D bioprinter [8].

In order to create more mechanically stable structures, collagen could be combined with alginate as it provides fast ionic crosslinking in calcium chloride or calcium sulfate solutions and is structurally stable with a wide range of concentrations offering superior mechanical properties [53,59]. Alginate is a polysaccharide derived from algae or seaweed. It is composed of two repeating monosaccharides, L-guluronic and D-mannuronic acids. The ionic crosslinking process is reversible, so the printed structures cannot be maintained for long-term culture applications [84]. Due to its biocompatibility, low price and fast gelation rate, alginate has been extensively used as a bioink for extrusion-based bioprinting [59]. Alginate can be extruded either as a precursor or as a pre-crosslinked solution by mixing it with low concentrations of a crosslinker [85]. Droplet-based printing of alginate is also feasible as long as below 2% concentration is used allowing droplet formation [86]. In addition, laser-based bioprinting of alginate with different concentrations has been successfully tested [86,87]. Despite the advantageous features of alginate, cells are unable to interact with alginate matrix via surface receptors due to the highly hydrophilic nature of alginate. Thus, cells inside the alginate gel are immobilized and have limited proliferation capabilities. Improvement in cell adhesion, spreading and proliferation can be achieved by modifying alginate with cell adhesion ligands containing RGD sequence or using alginate in combination with collagen I [59]. A proprietary bioink called NovoGel® [55] is also based on alginate blended with gelatin. This thermo-responsive bioink has been successfully used to print liver tissue and kidney proximal tubule tissue models with extrusion-based NovoGen Bioprinter® Instrument (Organovo Inc., San Diego, CA) [54, 88].

Methylcellulose does not occur naturally, instead it is derived from cellulose by replacing hydroxyl residues with methyl groups. It is a linear chain of polysaccharide and can form hydrogel by thermoreversible mechanism below 37°C [56]. Methylcellulose can be used as bioink, although it requires a thermally controlled nozzle and a heating plate. Due to its unstable structure upon exposure to cell culture media, methylcellulose is not suitable for long-term cell culture [89, 90].

Hyaluronic acid (HA), also known as hyaluronan, is a linear nonsulfated glycosaminoglycan ubiquitous in almost all connective tissues [91]. It is widely used in tissue engineering due to its excellent biocompatibility, minor cross-species variation, and ability to form flexible hydrogels [57,58,92]. However, the poor mechanical properties, slow gelation and rapid degradation are the major disadvantages of hyaluronan as bioink [93]. The degradation rate can be controlled via chemical modification. Yet, due to the slow gelation and poor mechanical properties hyaluronic acid is not ideal bioink for extrusion-based bioprinting. Instead, it should be blended with other hydrogels to enhance its bioprintability and gelling rate. Due to hyaluronan's viscous nature and slow gelation rate, droplet-based bioprinting of hyaluronan has not been demonstrated yet [75]. Laser-based printing, however, has been successfully tried by combining hyaluronan with other hydrogels, such as fibrin, to accelerate crosslinking [94].

### *3.3. Decellularized extracellular matrix*

As none of the natural or synthetic hydrogel bioinks can mimic the natural ECM perfectly, tissue-specific decellularized hydrogels have been tested as bioinks. Kidney-specific ECM increases the proliferation and metabolic activity of the kidney stem cells compared with kidney cell cultures in the bladder- or heart-derived ECM [18]. However, kidney-derived hydrogels have not been used as bioinks yet [95]. There also exist several limitations related to the use of decellularized ECM (dECM) as bioinks. Since the dECM is obtained via decellularization of the natural organs, the achieved volume of dECM is quite small and a large volume of initial tissues is required to create enough tissue for bioprinting. This of course increases the costs of the bioink. dECM also loses its mechanical properties and structural integrity upon being crushed into small fragments, which calls for the need to use a separate structural frame to prevent the printed dECM structure from collapsing [59].

Given the complex nature of the renal ECM (reviewed in [96]) finding a bioink that will fulfill all the necessary criteria of 3D bioprinting, such as bioprocessability, biomimicry, biocompatibility, biodegradability, tissue fusion permissiveness, shape maintenance after printing, hydrophilicity, pro-angiogenicity, affordability and approvability by FDA (see Table 2), is a difficult task. However, many studies of mixing synthetic hydrogels (providing mechanical structure) with natural polymers (providing function) should be performed to find the best combination to support the 3D bioprinting of kidney.

## 4. Bioprinting techniques and printing strategies

3D bioprinting techniques can be classified into three different categories according to their working principle: extrusion-, droplet-, and laser-based bioprinting. The comparison of the 3D bioprinting techniques is collated in Table 3 and the differences between printing strategies are

depicted in Figure 1. A common feature for all of the bioprinter types is the utilization of computer-aided manufacturing (CAM) to generate a toolpath plan providing the motion path for the bioprinter to deposit bioink at proper time and location [97]. The toolpath can be created from a computer-aided design (CAD) model representing the architecture of a tissue construct, however, the current CAD-based modelling systems are highly time-consuming and computationally expensive platforms. Thus, image-based design approach, which directly utilizes medical images to generate the external anatomical shape of the tissue construct, has been widely used for the blueprint modelling. The medical image-based surface model is finally filled with repeating unit cells found from a database of porous architectures to generate the complete construct. As different bioprinters work by different mechanisms, the toolpath plan varies from printer to printer. As the toolpath is generated, it is translated into digital signals by the machine control software. These signals control the motion and the dispensing mechanisms. Deposition of cells is performed in a medium called the bioink using an external source of energy, such as a laser, mechanical, thermal, or pneumatic energy. A robotic system prints the cells by depositing the cell-containing bioink, which is then solidified and stacked layer-by-layer to yield a 3D structure [75].

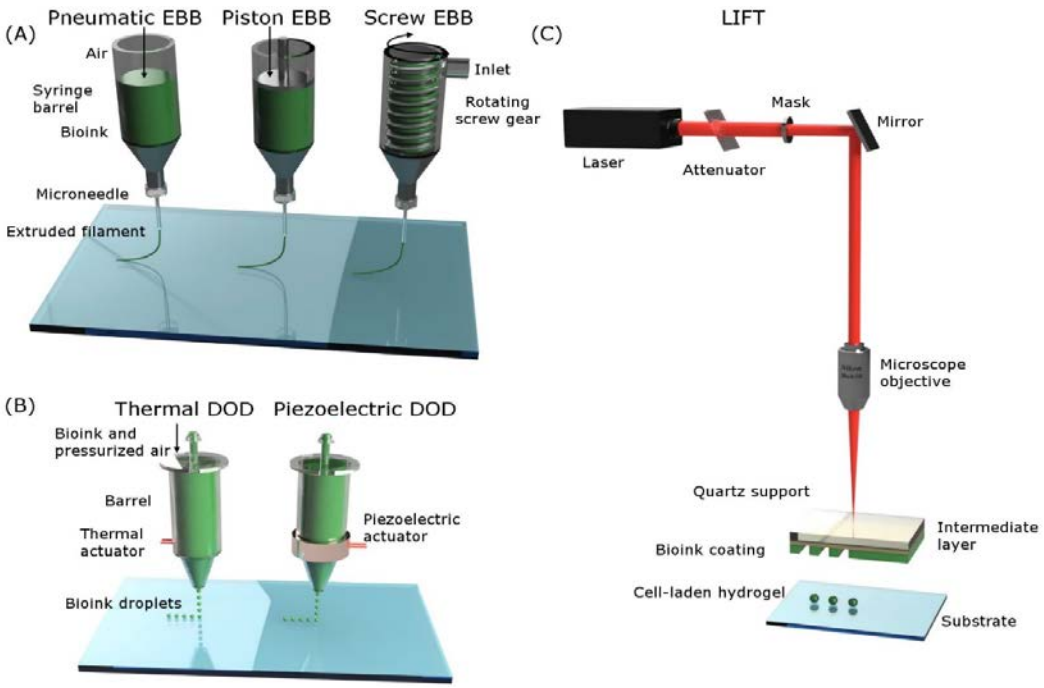


**Figure 1.** Different bioprinting techniques and their working principles. (A) Extrusion-based bioprinting (EBB) systems are driven by either air pressure, a piston or a rotating screw. Instead of droplets, a continuous filament of bioink is dispensed. (B) Thermal and piezoelectric drop-on-demand (DOD) inkjet printing systems. In thermal DOD printers, thermal actuator heats the bioink solution creating vapor bubbles, which in turn generate pressure pulse and force droplets out of the nozzle. In piezoelectric DOD printers, an actuator changes its shape producing a pressure wave, which ejects the bioink droplet. (C) Laser-induced forward transfer (LIFT) system, in which the laser is focused on an absorbing intermediate layer creating a vapor bubble. As the bubble expands, a jet of bioink is formed transferring bioink droplets onto a substrate.

**Table 1.** Protocols to generate nephron progenitor cells and ureteric bud progenitor cells.

| Cell source | Differentiation protocol | | | Generation of organoids | | | | | | Special notes | Ref. |
|---|---|---|---|---|---|---|---|---|---|---|---|
| | Dimensions | Length | Stages | % NPC | *in vitro* | Injection *in vivo* | Disease model | Place of injection | Therapeutic effect | | |
| *Nephron progenitor cells* | | | | | | | | | | | |
| hESC | 2D | 14–18 days | 1) Primitive streak – 2 days with BMP7/Activin A or CHIRR in serum free APEL medium,<br>2) Intermediate mesoderm – 6 days with FGF9 in serum free APEL medium,<br>3) UB & MM cells – 6 days in serum free APEL medium with no growth factors, but replated to low density | 10% Six2+ | yes | no | – | – | – | – | [27] |
| hiPSC | 3D | 14 days | 1) Embryoid body – 1 day with BMP4 in DMEM/F12 serum free medium,<br>2) Epiblast – 2 days with Activin A in DMEM/F12 serum free medium,<br>3) Nascent mesoderm – 2 days with BMP4 and CHIRR in serum free DMEM/F12 medium,<br>4) Posterior nascent mesoderm – 4 days with BMP4 and CHIRR in serum free DMEM/F12 medium,<br>5) Posterior intermediate mesoderm – 2 days with Activin A/BMP4/CHIRR in serum free DMEM/F12 medium,<br>6) MM cells – 3 days with CHIRR & FGF9 in serum free DMEM/F12 medium | 62% Six2+ | yes | no | – | – | – | – | [28] |

*Continued on next page*

| Cell source | Differentiation protocol | | | | Generation of organoids | | | | | Special notes | Ref. |
|---|---|---|---|---|---|---|---|---|---|---|---|
| | Dimensions | Length | Stages | % NPC | *in vitro* | Injection *in vivo* | Disease model | Place of injection | Therapeutic effect | | |
| hiPSC | 2D | 21 days | 1) Primitive streak – 1 day with Activin A & Wnt3a and 2 days with BMP4 & FGF2 in a RPMI medium,<br>2) Intermediate mesoderm – 8 days with BMP7 & FGF2 & RA in RPMI medium,<br>3) Nephron progenitors – 15 days with BMP7 and FGF2 in RPMI medium | 38% Six2+ | No | No | – | – | – | – | [29] |
| hiPSC | 2D & 3D | 28 days | 1) Embryoid body (3D) – 3 days with Activin A & CHIRR in DMEM/F12 medium,<br>2) Mesendoderm (2D) – 3 days with BMP7 & CHIRR in DMEM/F12 medium,<br>3) Intermediate mesoderm (2D) – 5 days with TFGB1 & TTNBP in DMEM/F12 medium,<br>4) MM cells (2D) – up to 17 days with TGFb1 & DMH1 in DMEM/F12 medium | 32.8% Six2/ Osr1+ | yes | yes | IR model of AKI | Kidney capsule | yes | – | [30] |
| hiPSC | 2D | 7 days | 1) Intermediate mesoderm – 4 days of CHIRR in serum free APEL medium,2) UB & MM cells – 3 days with FGF9 in serum free APEL medium | – | yes | no | – | – | – | Cisplatin nephrotoxicity tested | [31] |

*Continued on next page*

| Cell source | Differentiation protocol | | | | Generation of organoids | | | | | Special notes | Ref. |
|---|---|---|---|---|---|---|---|---|---|---|---|
| | Dimensions | Length | Stages | % NPC | *in vitro* | Injection *in vivo* | Disease model | Place of injection | Therapeutic effect | | |
| hPSC | 3D & 2D | 5 days | 1) Epiblast (3D) – 1 day with Rock inhibitor in TeSR medium, 1 day in Matrigel™ forming spheres in TeSR medium, and 1 day suspended in a TeSR medium,<br>2) Mesenchyme (2D) – 1.5 days with CHIRR in RPMI medium | – | yes | no | – | – | – | Cisplatin and gentamycin nephrotoxicity tested,<br>Modeled PKD | [32] |
| hiPSC | 2D | 3 days | 1) Primitive streak – 4 days with CHIRR & Noggin in advanced RPMI medium,<br>2) Intermediate mesoderm – 3 days with Activin A in advanced RPMI medium,<br>3) Nephron progenitors – 2 days with FGF9 in advanced RPMI medium | 32% Six2+ | yes | no | – | – | – | Cisplatin and gentamycin nephrotoxicity tested | [33,34] |
| hPSC | 2D | 12 days | 1) Intermediate mesoderm – 3 days with CHIRR in serum free APEL medium,<br>2) UB & MM cells – 9 days with FGF9 & Heparin in serum free APEL medium | – | yes | yes | no | Subcutaneously | – | Teratoma formation tested | [21] |
| *Ureteric bud progenitor cells* | | | | | | | | | | | |
| hiPSC | 2D | 4 days | 1) Mesoderm – 2 days with BMP4 and FGF2 in DMEM/F12 medium,<br>2) Intermediate mesoderm – 2 days with Retinoic Acid, Activin A and BMP2 in DMEM/F12 medium,<br>3) UB cells – 2 days in mTeSR medium | – | yes | no | yes | – | – | Modeled PKD | [35] |

**Table 2.** Types and properties of bioinks.

| Bioink type | Name of the polymer | Characteristics of an ideal polymer for kidney printing | | | | | | | | | | Printing methods | Gel transition method | Advantages | Disadvantages | Ref. |
|---|---|---|---|---|---|---|---|---|---|---|---|---|---|---|---|---|
| | | 1 | 2 | 3 | 4 | 5 | 6 | 7 | 8 | 9 | 10 | | | | | |
| Synthetic | Polyethylene glycol diacrylate (PEGda) | + | − | + | − | − | + | + | − | + | + | Extrusion, droplet-based, and laser-based | Photopoly-merization | Non-immunogenic, high transparency, tunable mechanical properties, functionalizable with various ligands | Potential cytotoxicity caused by UV-irradiation, low cellular adhesiveness, and cell proliferation | [48] |
| | Polyacryl-amide (PAAm) | + | − | + | − | − | + | + | − | + | + | Extrusion | Covalent crosslinking | Tunable stiffness | Toxic monomer, nondegradable | [49] |
| | Pluronic® F127 | + | + | + | + | + | + | + | − | + | + | Extrusion | Thermal crosslinking | High printability, nonimmunogenic | Poor mechanical and structural properties, rapid degradation | [50] |
| Natural | Fibrin/ Gelatin | + | + | + | + | + | + | + | + | − | + | Extrusion and droplet-based | Enzymatic crosslinking (fibrin), thermal crosslinking (gelatin) | Gelatin: cell-adherent, biocompatible, nonimmunogenic; Fibrin: proangiogenic, fast gelation, good integrality; Blend: good printability, ECM-like stiffness and composition, long-term stability | Gelatin: unstable, fragile, weak mechanical properties at physiological temperature and poor printability without modification; Fibrin: immunogenic, poor shape stability, low mechanical properties, limited extrusion printability | [50] |

*Continued on next page*

| Bioink type | Name of the polymer | Characteristics of an ideal polymer for kidney printing | | | | | | | | | | Printing methods | Gel transition method | Advantages | Disadvantages | Ref. |
|---|---|---|---|---|---|---|---|---|---|---|---|---|---|---|---|---|
| | | 1 | 2 | 3 | 4 | 5 | 6 | 7 | 8 | 9 | 10 | | | | | |
| | Matrigel™ | ± | ± | + | + | + | − | + | + | − | − | Extrusion and laser-based | Thermal crosslinking | Promotes cell differentiation and vascularization of construct, supports cell viability, good bioprintability | Batch-to-batch variation, slow gelation, which affects mechanical stability, requires cooling system for EBB, expensive | [32,51] |
| | Collagen 1 | ± | + | + | + | + | − | + | + | − | + | Extrusion, droplet-based, and laser-based | pH-mediated and thermal crosslinking | High cellular adhesiveness and promotion of cell migration and proliferation, nonimmunogenic | Fast degradation due to cellular remodeling, slow gelation, relatively low mechanical integrity | [52] |
| | Alginate | + | − | + | + | + | + | + | − | + | + | Extrusion, droplet-based, and laser-based | Ionic crosslinking | Low cost, rapid gelation, nonimmunogenic | Lack of biomimicry, low cellular adhesiveness, and limited cell proliferation and interaction | [53–55] |
| | Methyl cellulose | + | − | + | + | + | + | + | − | + | + | Extrusion | Thermal crosslinking | High printability, biocompatible, nonimmunogenic | Sensitive to cell culture media, unstable | [56] |
| | Hyaluronic acid | ± | + | + | + | + | − | + | + | − | + | Extrusion and laser-based | Ionic or covalent crosslinking | Promotion of cell migration, proliferation and angiogenesis, nonimmunogenic | Slow gelation, rapid degradation, low mechanical properties and stability without modification | [57,58] |
| Decellu-larized organ | Kidney | ± | + | + | + | + | − | + | + | − | + | Extrusion | Thermal crosslinking | Biomimetic, promotion of cell differentiation, proliferation, and long-term functionality | Slow gelation and lack of mechanical properties | [44] |

Note: An ideal polymer for kidney bioprinting should fulfill all 1–10 criteria, which are as follows: 1—bioprocessable (dispersible and fast solidification), 2—biomimetic (similar to the one occurring in the organ of choice), 3—biocompatible (nontoxic, promoting high cell viability), 4—biodegradable (removable on demand), 5—tissue fusion permissive (optimal physicochemical properties, such as the suitable stiffness and removability immediately after tissue fusion), 6—shape-maintaining (preventing construct from melting and distortion), 7—hydrophilic (promoting efficient diffusion), 8—pro-angiogenic (permissive for cell attachment, migration and proliferation as well as providing for host vasculature), 9—affordable (relatively low cost), 10—FDA approvable (non-cancerogenic and non-immunogenic).

**Table 3.** Comparison of different 3D bioprinting techniques.

| Bioprinting technique | Additive unit | Printer modality/ Actuation method | Nozzle configuration/ Working principle | Advantages | Disadvantages | Ref. |
|---|---|---|---|---|---|---|
| Extrusion-based bioprinting | Cylindrical filaments | Pneumatic pressure | Valve-free | Simple, widely used in commercial bioprinters, suites for hydrogels with shear-thinning properties | Low viscosity hydrogels may flow through the nozzle | [59] |
| | | | Valve-based | Suites for high precision applications and low-viscosity bioinks | | |
| | | Mechanical pressure | Piston-driven | Better control over the flow of bioink through the nozzle, suitable for dispensing fluids with low viscosity | | [6] |
| | | | Screw-driven | Good spatial control, capable of generating high pressure for dispensing bioinks with higher viscosities | Requires cleaning of mechanical parts, high pressure can be harmful to the loaded cells | |
| | | Solenoid pulse | Ferro-magnetic plunger | Enables dispensing of sub-μL droplets, suitable for low-viscosity bioinks | Number of factors affecting the accuracy and reproducibility | [75] |
| Droplet-based bioprinting | Droplet | Thermal DOD | Microheating element for creating bioink vapor bubbles | Affordable, ideal for feasibility studies | Thermal stress (200–300°C) on cells during droplet formation, difficult to clean as cartridges are designed for paper printing (2D) | [41,75] |
| | | Piezoelectric DOD | Rapid shape change of a piezoelectric material creates a pressure wave | Good control over droplet shape and size, wide variety of inks can be printed as the ink does not have to be volatile | Nozzle clogging, satellite droplets, mechanical stress on cells during droplet ejection | [41,75] |

*Continued on next page*

| Bioprinting technique | Additive unit | Printer modality/ Actuation method | Nozzle configuration/ Working principle | Advantages | Disadvantages | Ref. |
|---|---|---|---|---|---|---|
| | | Electrostatic DOD | Temporarily increase of the fluid chamber volume by deflecting a pressure plate | Affordable, ideal for feasibility studies | Limited cell types and clogging issues due to small nozzle diameter, mechanical stress on cells during droplet ejection | [75,98] |
| | | Elecrohydro-dynamic jetting | Voltage pulses generate electric field between the nozzle and the substrate | Capable of dispensing droplets of < 10 μm in size, low mechanical stress on cells during droplet formation, capable of dispensing viscous bioinks | Expensive, complete systems commercially unavailable, unsafe for the operator, unable to eject single droplets | [99,100] |
| | | Acoustic bioprinting | Ultrasound field ejects droplets from an air-liquid interface | Uniform droplet size and ejection directionality, no nozzle clogging or mechanical stress on cells | Viscous bioinks with high cell concentrations are not dispensable, unavailability of complete commercial systems | [41,101] |
| | | Microvalve bioprinting | Electromechanical microvalves generate droplets by opening and closing due to an applied air pressure | Affordable, capable of dispensing viscous bioinks, interchangeable nozzles | Larger droplets as compared to other DBB methods yielding to a lower resolution | [75,102] |
| Laser-based bioprinting | Cured bioink voxel | Photopolymerization-based SLA | An UV-laser solidifies the photosensitive bioink placed in a vat equipped with a porous motorized table | Tissue constructs ranging in size from a few hundred micrometers to a few millimeters can be bioprinted, intermediate fabrication times | Cytotoxic photoinitiators, low resolution as it depends on the exposure conditions and on the photosensitive material, limited choice of bioink materials | [41,103] |
| | | Photopolymerization-based DOPsL | Solidification through a digital mask projected onto the surface of the photosensitive bioink | Shorter fabrication times, enables fabrication of scaffolds with complex internal architecture | Limited selection of bioink materials, limited control on the layer thickness | [41,75,104] |

*Continued on next page*

| Bioprinting technique | Additive unit | Printer modality/ Actuation method | Nozzle configuration/ Working principle | Advantages | Disadvantages | Ref. |
|---|---|---|---|---|---|---|
| | | Photopolymerization-based 2PP | Tightly focused pulsed laser beam is scanned in the volume of the photosensitive bioink with a mirror scanner | Features with line width beyond the diffraction limit ( < 100 nm) can be fabricated | Not suitable for cell encapsulation unless water-soluble photoinitiators are used, cell viability of only 25% around laser-exposed regions | [105,106] |
| | Droplet | Cell transfer-based LGDW | Laser-induced pulse entraps cells due to gradient forces and propels them towards a substrate | High resolution, high cell viability due to only weakly focused laser beam | Quite slow printing speed, viscous bioinks are not printable | [75,107] |
| | | Cell transfer-based MAPLE-DW | Laser fluence is used to generate plasma bubbles that eject the coating material to a substrate | Viscous bioinks can be printed, nozzle-free transfer of cells | Thermal stress on cells, long fabrication times due to manual preparation of the ribbon, low cell viability at higher laser fluence, simultaneous deposition of multiple bioinks is difficult | [75] |
| | | Cell transfer-based LIFT | Similar to MAPLE-DW, but an energy-absorbing IR-transparent interlayer is used | Minimal effects of the laser exposure to cells, viscous bioinks can be dispensed | Long fabrication times due to manual ribbon fabrication, simultaneous deposition of multiple bioinks is difficult | [108] |

### *4.1. Extrusion-based bioprinting*

Extrusion-based bioprinting (EBB) has evolved from fused-deposition modeling (FDM), which was invented by Scott and Lisa Crump, the founders of Stratasys, in 1988 [109]. Since the expiration of the original FDM patent in 2009, the global market has been opened for material extrusion. The technique was adapted in 2002 for tissue engineering purposes to print porous scaffolds, i.e. temporary housings for cells [110]. Later, extrusion-based printing technique has been started to be used for bioprinting of cell-aggregates on hydrogel biopaper surfaces [111]. EBB functions by robotically controlled extrusion of material, which is dispensed as cylindrical filaments onto a substrate by an extrusion head. The dispensing system can be driven by a pneumatic-, mechanical-, or solenoid-based system to overcome surface tension-driven droplet formation and draw the bioink in the straight filament form. Pneumatic-based system uses pressurized air via valve-free or valve-based configuration. The mechanical dispensing system is based on either a piston or screw-driven configuration [6,59]. In general, EBB is very versatile and affordable printing method, and it has greater deposition and printing speed than other methods, which facilitates the scalability of the technique. Also, several commercial EBB printers are already available [75]. EBB is the only bioprinting method allowing printing of high cell densities with reasonably small process-induced cell damage. However, the resolution of the EBB technique is very limited as the minimum feature sizes are generally over 100 μm [36], which is considerably inferior to other bioprinting techniques, especially laser-based bioprinting [112]. The poor resolution makes it impossible to pattern the cells precisely thus limiting the applicability of EBB systems. Although the resolution could be improved by using smaller nozzle sizes, this would unfortunately also increase the shear stress and stress-related cell death [75].

### *4.2. Droplet-based bioprinting*

Droplet-based bioprinting (DBB) relies on either thermal, acoustic or electric energy to print cells encapsulated in the small droplets of bioink. Droplet techniques can be further categorized into four groups: inkjet, electrohydrodynamic jetting, acoustic droplet ejection, and microvalve bioprinting. Furthermore, inkjet bioprinting can be classified into continuous inkjet (CIJ) and drop-on-demand (DOD) inkjet printing systems, and drop-on-demand inkjet systems are divided into thermal, piezoelectric, and electrostatic printers [75]. The inkjet bioprinting originated from commercial 2D inkjet printing [113]. The idea of printing biological components was developed by Klebe in 1987, when he used a commercially available Hewlett-Packard thermal inkjet printer to deposit collagen and fibronectin [114]. Furthermore, in 2003 Boland used a modified thermal inkjet printer to deposit living cells [113], thus introducing the concept of inkjet bioprinting [115]. In fact, the necessary equipment for DBB can be easily remodified from a 2D inkjet desktop printer, making this technique widely available for researchers worldwide and relatively inexpensive [41].

CIJ bioprinters are based on forcing the bioink solution under pressure through a small diameter orifice, and the resulting jet breaks up into a stream of droplets due to the Rayleigh-Plateau instability phenomenon [116]. In this physical phenomenon, a thread of jet breaks up into droplets in

order to minimize its surface tension [75]. DOD bioprinters operate similarly to the traditional 2D inkjet printers, i.e. drops are generated only when required by propagating a pressure pulse in a fluid filled chamber [116]. DOD bioprinters are preferred over CIJ bioprinters for tissue engineering purposes. In models relying on thermal actuation, the bioink is heated with a microheating element to create vapor bubbles. When the vapor bubble collapses, an acoustic pressure pulse is generated for ejecting the droplets. In piezoelectric actuation, a rapid change in the shape of a piezoelectric material generates a pressure pulse in the fluid forcing a droplet out of the nozzle [41]. Electrostatic bioprinters are identical to piezoelectric printers and they form droplets by temporarily increasing the volume of the fluid chamber by deflecting a pressure plate with a voltage pulse applied between the plate and an electrode [98]. In the electrohydrodynamic jet bioprinting, an electric field generated between a positively charged needle and a negatively charged substrate pulls the bioink droplets through the orifice [99,100]. Acoustic bioprinting employs a gentle ultrasound field to eject droplets from an air-liquid interface of an open pool. Acoustic radiation is capable of ejecting cells from an open pool without clogging the nozzle or damaging the cells, however, viscous hydrogels with high cell concentrations may not be printed [41,101]. Microvalve bioprinters use a set of electromechanical microvalves consisting of a solenoid coil and a plunger to generate droplets by opening and closing the valve via an applied air pressure [102]. When a voltage pulse is applied, the valve coil is magnetized and the plunger is pulled upwards thus unplugging the nozzle. Generally, microvalve bioprinters dispense larger droplets as compared to other DBB methods yielding to a lower resolution [75].

### *4.3. Laser-based bioprinting*

Stereolithography (SLA) is the oldest 3D printing technology; it was invented by Charles W. Hull, who patented the technique in 1985. It allows for the fabrication of arbitrarily shaped structures in assembly-free manner by focusing an ultraviolet light on a spot in a photosensitive liquid enabling selective solidification of the material according to predefined path [117]. Although SLA has been used for the fabrication of tissue scaffolds, living cells have generally been seeded on the scaffolds after printing. In 2004, Boland and his coworkers used a commercially available SLA system to bioprint human cells and succeeded in fabricating highly complex scaffolds that cannot be fabricated using EBB or DBB modalities [118]. However, 2D patterning of living cells using laser-assisted technology was introduced already in 1999 by Odde and Rehn [119]. Since then, several groups have started to use laser energy for printing living cells [120–122]. The fabrication of 3D tissue constructs became feasible with the invention of laser-assisted bioprinting as an extension of matrix-assisted pulsed-laser evaporation (MAPLE). All of these laser energy based techniques can be classified under laser-based bioprinting (LBB) [75].

LBB is capable of fabricating highly accurate tissue constructs, but its intricate setup has limited its commercialization; currently there exists only one company worldwide using LBB for the fabrication of tissues and no LBB setups capable of printing living cells have yet been commercialized. However, various research groups have acquired components of the LBB setups and built their own customized printers. LBB techniques can be classified into two major subclasses including processes involving photopolymerization and processes based on cell transfer. Furthermore,

photopolymerization processes include SLA, dynamic optical projection stereolithography (DOPsL), and two-photon polymerization (2PP). Cell transfer processes can be further classified either as laser-guidance direct writing (LGDW), matrix-assisted pulsed laser evaporation-direct write (MAPLE-DW), or as laser-induced forward transfer (LIFT) [75]. DOPsL is a maskless printing method, where a digital mask is projected onto the surface of the photocurable bioink using a digital light procession technique allowing the solidification of the entire bioink layer at once [41,104]. See Table 3 for more details on each type of LBB printing.

The overall resolution of SLA depends on the focal spot size and is limited by diffraction, which in theory should result in feature sizes equal to half of the applied laser wavelength. In practice, the achieved resolution is in the range of a few micrometers [103,123]. The resolution can be improved by using 2PP technique, where a tightly focused pulsed laser is used to initiate polymerization reaction within the focal volume as the photoinitiator molecules absorb two photons simultaneously [106]. As 2PP is able to produce scaffolds with nanoscale resolution, it could be beneficial to couple it with some other bioprinting modality into a hybrid bioprinting platform, and use it for the fabrication of nanosize features to control cell adhesion.

LBB processes based on cell transfer offer the direct deposition of materials on a free surface based on the "aim-and-shoot" principle. The setups typically consist of a laser-absorbing metal layer coated on a laser transparent support, called the ribbon, a feeding layer of cell-laden hydrogel beneath, and a receiving substrate. During the aim step, a laser pulse is focused on the laser-absorbing layer and a vapor pocket is generated in the feeding layer resulting in the formation and transfer of the cell-containing droplet from the ribbon to the receiving substrate (the "shoot" step) [124].

LGDW was the first LBB technique used for bioprinting of living cells [119]. MAPLE technique was developed at the US Naval Research Laboratory in the late 1990s. The organic compound is first dissolved in an alcohol solvent and the solution is frozen at -196°C to form a laser target. The solvent toxicity makes it impossible to encapsulate living cells within the matrix and the cryogenic setup is not hospitable environment for cells. Thus, the technique was further modified by encapsulating cells into a bioink solution and by forming a thin coating of the hydrogel on the bottom side of the print ribbon. The new method was called MAPLE-DW, in which a range of laser fluences below the ablation threshold of the bioink material is used to generate plasma bubbles that eject the bioink to a substrate [75]. In an advanced version of MAPLE-DW, called LIFT, cells are also encapsulated in coating material and are transferred to a substrate, which is in close proximity with the coating material. In contrast to MAPLE-DW, in LIFT, an energy-absorbing IR-transparent interlayer is used to diminish the detrimental effect of the intensive UV light to cells [108]. As nozzle-free approaches, LBB techniques circumvent several limitations that EBB and DBB techniques face, such as the shear stress-induced cell damage or nozzle clogging. The major advantage of LBB is its high resolution, being below 10 μm in its best [125].

Despite the high resolution, processes based on photopolymerization suffer from prolonged fabrication times, the interaction of cells with damaging laser light, expensive setup prices, and lack of photocrosslinkable bioink choices. On the other hand, cell transfer-based processes face challenges due to laser shock related thermal- and mechanical induced cell deformation, the random placement of cells in the precursor solution, and expensive fabrication setups [75].

## 5. State-of-the-art in bioprinting of kidneys

Currently, the fabrication of a complex and large-scale 3D kidney is not possible. Hence, the research has been focused on 3D bioprinting of small-scale structures based on mini-tissue building blocks. Organs, such as kidney, consist of these smaller, functional building blocks, which can be defined as the smallest structural and functional component of the organ, such as a nephron. Mini-tissues, or more specifically tissue spheroids, can be fabricated and assembled into larger constructs via natural tissue fusion process or directed tissue self-assembly. In this scaffold-free approach, macrotissues can be achieved without any instructive, supporting, and directing solid scaffold simply by using tissue spheroids of different compositions and organizations as the bioink, which is bioprinted using layer-by-layer placement on tissue fusion permissive hydrogel (the biopaper) [126]. To bioprint organs, such as the kidneys, in clinically relevant volumes, EBB modalities are preferred over DBB and LBB methods. In fact, EBB enables bioprinting of various types of bioink materials, such as cell spheroids [127], cell-laden hydrogels [128], microcarriers [129], and decellularized matrix components [130], whereas other techniques only facilitate printing of cell-laden hydrogels.

Small-scale functional renal tissue structure has been recently achieved at Harvard's Jennifer Lewis' Lab as the researchers re-created a proximal tubule segment of a nephron [50]. 3D convoluted proximal channels were bioprinted using a custom-made EBB setup equipped with four independently addressable printheads mounted onto a 3-axis, motion-controlled gantry. Inks were housed in separate syringe barrels to which nozzles varying in sizes from 50 μm to 410 μm were attached. Air pressure was used to deposit materials through nozzles. 3D proximal tubule was fabricated within a perfusion chip by first casting a base ECM layer (fibrinogen & gelatin) on the bottom of the perfusion chip, and then printing the fugitive Pluronic® F127 ink on the base in the form of a convoluted tubule. The top layer of ECM was then cast over the printed tubule. Finally, the temperature was lowered to 4°C to liquefy the fugitive ink leaving behind the open conduits, which were seeded with human immortalized proximal tubular cells.

The tissue engineering company Organovo Inc. (San Diego CA, USA) has partnered with the Murdoch Children's Research Institute for bioprinted kidney research. It has generated kidney tissue constructs (3D PT ExVive™ Human Kidney Tissue) for compound screening and disease modeling by using their proprietary 3D bioprinting platform (http://organovo.com/tissues-services/exvive3d-human-tissue-models-services-research/exvive-kidney-tissue/) The construct is a fully cellular human *in vitro* model of the proximal tubule interstitial interface. Cultured renal fibroblasts and human umbilical vein endothelial cells (HUVECs) are suspended in thermos-responsive NovoGel® Bio-Ink and bioprinted with NovoGen Bioprinter® Instrument (Organovo Inc., San Diego, CA) onto polyester membrane inserts in a 24-well plate [54,88]. The bioprinting is based on mechanical extrusion from multiple nozzles. After three days in culture, primary renal proximal tubule epithelial cells (RPTECs) are seeded on the printed tissues to form an apical monolayer on top of the basal multicellular interstitial layer composed of primary human renal fibroblasts and HUVEC cells [54].

Also, Anthony Atala's group at the Wake Forest Institute for Regenerative Medicine (Winston-Salem, NC, USA) has been working towards bioprinting of transplantable kidneys. In fact, they have already successfully printed an early stage kidney prototype using an EBB setup called Integrated Tissue-Organ Printer (ITOP) [6]. The ITOP system is capable of bioprinting

multiple materials at the same time, such as cell-laden composite hydrogels, supporting poly (ε-caprolactone) (PCL) polymer, and sacrificial Pluronic® F127 hydrogel. The system consists of three major units: three-axis motorized stage, dispensing module with multiple air-pressure controlled microscale nozzles combined with cartridges, and a closed acrylic chamber for temperature and humidity control. In addition, one of the nozzles is equipped with a heating unit for dispensing PCL [131].

Just like Organovo's Novogen Bioprinter®, the FABION 3D bioprinter developed by 3D Bioprinting Solutions (Moscow, Russia) is targeted exclusively for internal use. Their objective is to print a functional and implantable human organ in the near future. In fact, they are currently co-operating with the University of Oulu and 3DTech Oy to bioprint a mini-kidney using kidney organoids (https://3dprint.com/181528/3d-bioprinting-solutions-thyroid/). As a proof of concept, the company has already printed functional thyroid glands and transplanted them into mice [8]. FABION is equipped with five deposition nozzles allowing precise dispensing of tissue spheroids in hydrogel biopaper. Three nozzles are for dispensing bioink consisting of spheroids, cell suspension, or other materials. The number of tissue spheroids to be dispensed, the thickness of the printed layer and other parameters can be set independently for each nozzle. The other two nozzles are for dispensing biopaper, which can be polymerized by UV radiation (http://www.bioprinting.ru/en/investors/projects/fabion/).

Yet another company pursuing to bioprint functional kidney structures is Nano Dimension Ltd.'s subsidiary Nano Dimension Technologies Ltd. (Israel). It has filed an U.S. patent application for 3D inkjet printing of living cells and supporting structures for the fabrication of nephron-like functioning structures. Their inkjet printing platform is capable of bioprinting multiple materials almost in parallel and on a wide area, which could make it suitable for the fabrication of complex tissue structures. Their initial plan is to 3D print structures composed of biomembranes that are composed of a few cell layers with each cell in direct contact with the blood supply (https://www.engineering.com/3DPrinting/3DPrintingArticles/ArticleID/14380/From-3D-Printing-Circuit-Boards-to-Organs-Nano-Dimensions-CEO-Discusses-New-Bioprinting-Subsidiary.aspx).

## 6. Challenges

Kidney is a rather big and quite complex organ to be printed as a whole at one attempt. The variety of cells required to complete this process, and size of the organ make this task very difficult. Therefore, the only way to approach is to 3D bioprint small pieces, mini-tissue building blocks, which could be put together after printing to form bigger organ. Both of these challenges, the size of the organ and the variety of cells, could be tackled by using organoids for printing (see the next chapter "7. Possible solution–vision of the 3D bioprinting of the kidney"). However, there are far greater challenges to be solved first, such as the vascularization of the kidney and the essential ductal system to drain the urine out, both of which are essential to provide the function/functionality to the organ.

### *6.1. Vascularization*

Vascularization or printing of vascularized organs is one of the most important and still unsolved problems in tissue engineering and 3D bioprinting technology. It is obvious that only well vascularized bioprinted thick tissues and organs could survive after implantation. There are several excellent reviews on the significance of vascularization in tissue engineering [132–136], all of which highlight the need for the appropriate perfusion of the vascular network and the generation of an adequately dense system to limit the distance between capillaries to the required 200 μm. Moreover, it has been shown that the progression of the chronic kidney disease (CKD) depends on the remodeling of the vascular network [23]; therefore, the correct vasculature in newly engineered kidneys is important for the later health of the recipient.

During the last decade, several promising technological breakthroughs have been achieved, but still there is no clear and realistic vision on how the bioprinted kidney could be effectively vascularized. This unsolved problem of the vascularization remains as the main impediment on our way to bioprint functional human kidney. In the case of the kidney, the vascularization is especially important because it plays a crucial role in two main kidney functions, i.e. in filtration and reabsorption, which are intimately connected with blood flow.

Theoretically, kidney vascularization could be implemented by two main ways: it could be either done after implantation using sprouting angiogenesis from the pre-existing vasculature of host organism or generated in the bioprinted kidney by vasculogenesis from endothelial progenitors before implantation. Indeed, it has been demonstrated that the kidney organoids can be effectively vascularized and even enable glomerulogenesis after implantation under a highly vascularized kidney capsule [19,20] or subcutaneously [21]. Moreover, the omentopexy or vascularization of an organ by mobilization and attachment to highly vascularized and angiogenic omentum tissue is a standard surgical practice [137,138]. However, such approach is effective only in the case of transplantation of the relatively small volume of renal tissue, such as the developing metanephroi [138]. Even though the metanephros undergoes vascularization by the host and develops mature and filtering glomeruli, it is not realistic to create a kidney with an intra-organ hierarchically branched vascular system including large diameter vascular segments suitable for surgical suturing using only sprouting angiogenesis from the recipient organism.

However, the development of renal vasculature from an intrinsic population of endothelial progenitors has been reported in many publications [139–144]. Nevertheless, only the early steps of renal vascularization, preceding the formation of glomerular tuft, could occur in the absence of blood flow [139,145]. It was shown that blood circulation is crucial for the formation of vascularized mature glomeruli [146], which is in agreement with the data obtained with transplanting renal organoids [19–21]. Therefore, in order to enable the glomerular vasculature formation, the flow of culture medium through perfused endothelial vessels has to be provided to the bioprinted kidneys, for instance by the means of microfluidics.

Rapidly developing microfluidic technology allows to biofabricate vascularized mini-tissues [147,148]. Microfluidic technology has, for example, been successfully used to biofabricate vascularized tumor spheroids [149]. It opens a realistic possibility to generate vascularized human kidney organoids using human endothelial cells. Vascularized kidney organoids could be a powerful research tool for studying human nephrogenesis and glomerulogenesis in a real time at single-cell resolution. Moreover, the implementation of automation and robotization will

enable scalable biofabrication of vascularized human nephrons sufficient for the bioprinting of human kidney. However, this approach has only started to be explored and certain time is needed for its successful realization, especially in a large scale.

Introduction of the concept of sacrificial (or removable) hydrogels opens a new interesting approach for vascularization of thick 3D tissues and organs by creating tunnels in the 3D bioprinted tissue constructs, which could be seeded with endothelial cells after removal of the sacrificial hydrogels [78,150,151]. However, this approach has two main limitations. It works very well for biofabrication of small diameter microvascular networks but it does not allow creating the relatively thick wall of large diameter vessels, which could be surgically connected with the recipient's large arteries. Currently, it is also not clear how the vascularized parenchyma of the kidney could be bioprinted using this approach. Most recently, by using the sacrificial hydrogel technique, functional kidney tubules have been bioprinted by the Jennifer Lewis' group, however, without the glomeruli and the surrounding microvessels [50].

Another elegant and potentially promising approach for kidney vascularization has been recently introduced by Anthony Atala's group [152]. The sacrificial vascular corrosion casts of intra-organ kidney vascular systems were used as a temporal support for the biofabrication of a collagen-based hydrogel coating of a tubular scaffold, biomimicking the kidney vascular system. After the removal of the corrosion casts, the collagen hydrogel generated a branched tubular system that was coated with endothelial cells. It remains to be seen how the parenchymal renal tissue could be incorporated and bioprinted around this vascular construct. From the technical point of view, it is practically impossible to bioprint a kidney organ construct inside already existing 3D vascular construct. The robotic placing of mini-tissues or tissue mini-blocks needs an open space, but the pre-existing 3D scaffold does not allow the implementation of this approach. It is also unknown, if the material properties of large diameter segments, such as the artificial kidney vascular constructs, are strong enough for surgical suturing. 3D bioprinting of the intra-organ branched vascular system and the parenchymal tissue must be made simultaneously using the general principles of layer-by-layer additive biofabrication.

Thus, the main challenge in solving the problem of vascularization of bioprinted kidney is not just bioprinting of multiple kidney nephrons and small kidney fragments or kidney tissue modules with microvascular network. Instead, the major challenge involves the bioprinting of a kidney construct with a built-in intra-organ hierarchically branched vascular system, including large diameter vascular segments suitable for surgical suturing.

### *6.2. Urine drainage system*

The main product of the functional activity of the kidney, the urine, is excreted through the sophisticated ductal system. The bioprinting of the complex renal ductal system is another unsolved challenge in 3D bioprinting of human kidney. The multiple attempts of tissue engineering (not 3D bioprinting!) of ureter, bladder and urethra are beyond the scope of this review and can be found elsewhere [153–156].

In the recent elegant study, it was demonstrated that *in vitro* tubulogenesis of Madin-Darby canine kidney (MDCK) spheroids occurs spontaneously when specific cell number (400–1500 cells)

and scaffold gel concentration (1–2%) are used [157]. MDCK cells form elongated tube structures through aggregation processes in these conditions, while in other conditions they are only able to form spherical aggregates. It is also interesting that cell proliferation is not required for the tube elongation. These results strongly suggest that the MDCK cells, during the aggregation process, interact with each other via mechanical forces transmitted by the scaffold gel, leading to the spontaneous tube formation. Thus, by combining proper cell concentration and hydrogel stiffness it is possible to biofabricate and perhaps even bioprint desirable tubular structures, which would mimic the authentic renal collecting tubes.

Anthony Atala's group reported for the first time about successful 3D bioprinting of urethra with biodegradable polymers and dual autologous cells in fibrin hydrogel [158]. In this study, the 3D bioprinting technology was used to fabricate cell-laden urethra *in vitro* with different polymer types and structural characteristics. PCL and poly(L-lactide-co-caprolactone) (PLCL) polymers and spiral scaffold design were chosen in order to mimic the structure and mechanical properties of natural urethra of rabbits. The cell-laden fibrin hydrogel was used in order to provide better microenvironment for cell growth. Using an integrated bioprinting system, tubular scaffold was formed from biodegradable polymers. The urothelial cells (UCs) and smooth muscle cells (SMCs) were delivered evenly into the inner and outer layers of the scaffold separately, within the cell-laden hydrogel. The PCL/PLCL (50:50) spiral scaffold demonstrated mechanical properties equivalent to the native urethra in rabbit. It was shown that the UCs and SMCs maintained more than 80% viability even at 7 days after printing. Both cell types also demonstrated proliferation and maintained the specific cell and tissue biomarkers. This shows that 3D bioprinting of urethral constructs, mimicking the mechanical properties and cell bioactivity of natural urethral tissue, is feasible [158]. Taken together these data provides a strong foundation for the future studies on 3D bioprinted urethra and other ductal systems, for example the one of the kidneys.

## 7. Possible solution—vision of the 3D bioprinting of the kidney

Adult kidney is a very complex organ consisting of millions of cells of hundreds different types. Bioprinting of individual cells is technically impossible at present and even if it would be possible, printing of such a complex morphological structure is an extremely challenging task. We suppose, that the fabrication of kidney by bioprinting will rely on utilizing the renal developmental program. Remarkable of the embryonic kidney is its potential for autonomous development *in vitro* [15,26]. Yet more intriguing is the potential of primary or even *in vitro* differentiated iPSCs to differentiate into renal cells to form functional nephrons by self-assembly in organoids [27,31,34]. Limitation of this potential, however, is inability of the renal structures to recapitulate the overall morphology of the kidney. Here, we propose to apply bioprinting to restore the overall order by the arrangement of different morphological units (nephrons, ureteric epithelium and vasculature) by the means of bioprinting.

While some challenges remain, we strongly believe that it is possible to 3D bioprint the kidney using tissue spheroids/organoids as building blocks for bioprinting; this strategy considers all required parts: the vasculature, the main kidney mass and the ductal system. For printing vasculature, this concept has already been outlined in several reviews and papers [159,160]. Moreover, several groups have bioprinted large diameter vascular segments suitable for surgical suturing [161–163].

Recently, we have introduced a novel concept of sacrificial vascular tissue spheroids, which enable the bioprinting of large lumenized vascular segments. The intermediate diameter vascular segments could be biofabricated and robotically bioprinted using lumenized vascular tissue spheroids [164,165]. The vascular network could then be formed from endothelial cells embedded in fibrin and collagen hydrogels by using the vascular endothelial growth factor (VEGF) [166–168]. Finally, the isolated segments of the vascular tree or endothelial spheroids have capability to fuse together into microvascular network *in vitro* and *in vivo* [169,170]. Thus, it is logical to assume that the combination of solid vascular tissue spheroids, sacrificial vascular tissue spheroids, lumenized vascular spheroids, endothelial spheroids and endothelial cells in bioprintable hydrogels will enable the bioprinting of complete built-in intra-organ hierarchically branched arterial and venous vascular systems consisting of the sequential segments of the vascular tree. Moreover, with rapid progress in the iPSC differentiation field, the endothelial cells for the 3D bioprinting of the vasculature could be derived from the patient's iPSCs [171].

When considering the kidney mass, the protocols to differentiate hPSCs/hiPSCs into NPCs and UBPCs (Table 1) already exist and therefore soon it might be possible to generate organoids containing only cells derived from patients. Moreover, these organoids may be able to fuse together upon printing in close proximity, just as the organoids derived from primary mouse MM cells do (Figure 2A), enabling the formation of larger complexes. The derivation of UBPCs from hPSCs/hiPSCs is also a promising technique, as it would enable avoiding the use of non-human cells (e.g., MDCKs) for printing the ureter structures.

Once 3D bioprinted, the small kidney unit and the vascular units, would have to be placed in a microfluidic chamber (Figure 2B) that would provide the flow and enable the functionalization of the kidneys. The bigger vasculature units would handle the main flow, and the flow would enable the rearrangement of the endothelial cells in close proximity to the kidney units, where they would form capillaries, which would enter the renal organoids and vascularize the developing glomeruli.

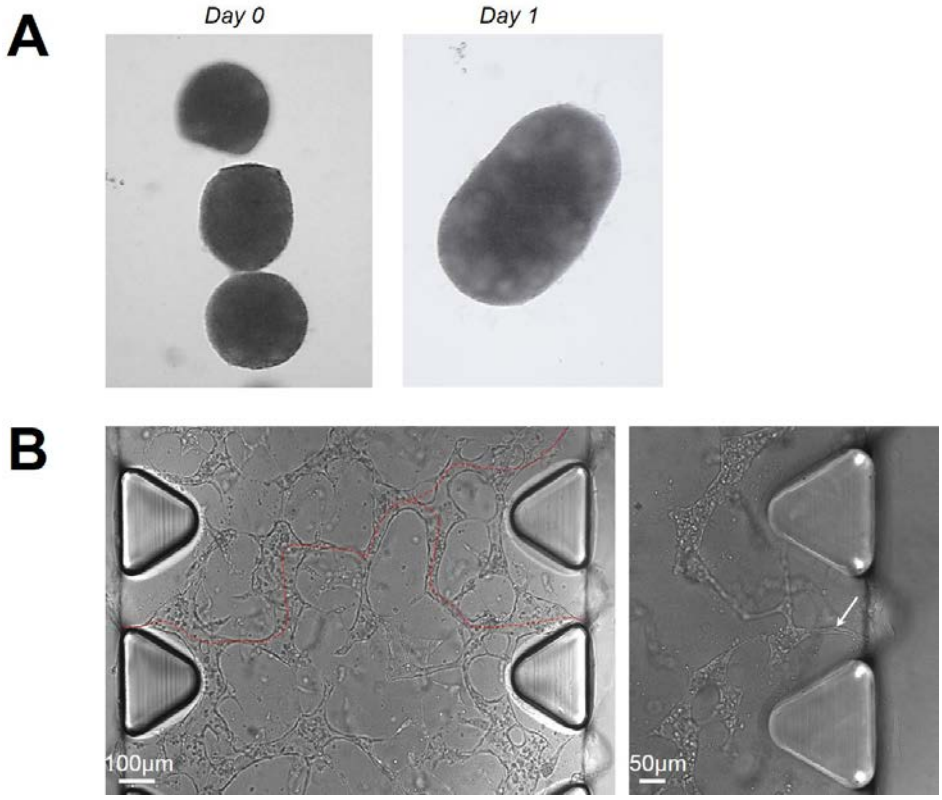


**Figure 2.** Possible technologies to 3D bioprint and functionalize the kidney. (A) Renal organoids generated from primary mouse MM cells, placed in close proximity to each other in Matrigel™ , fuse together already after 1 day of culture. (B) Left image: Microfluidic chamber with seeded HUVEC cells, which under the influence of an applied flow generate connections (red intercalated line), and in the right image, a flow outlet is marked with a white arrow.

## 8. Practical applications

While the main goal of the regenerative medicine is to enable production of rejection-free organs for transplantation, the smaller units of the 3D bioprinted functional kidneys may already be useful in other areas of biomedicine or pharmacology (Figure 3).

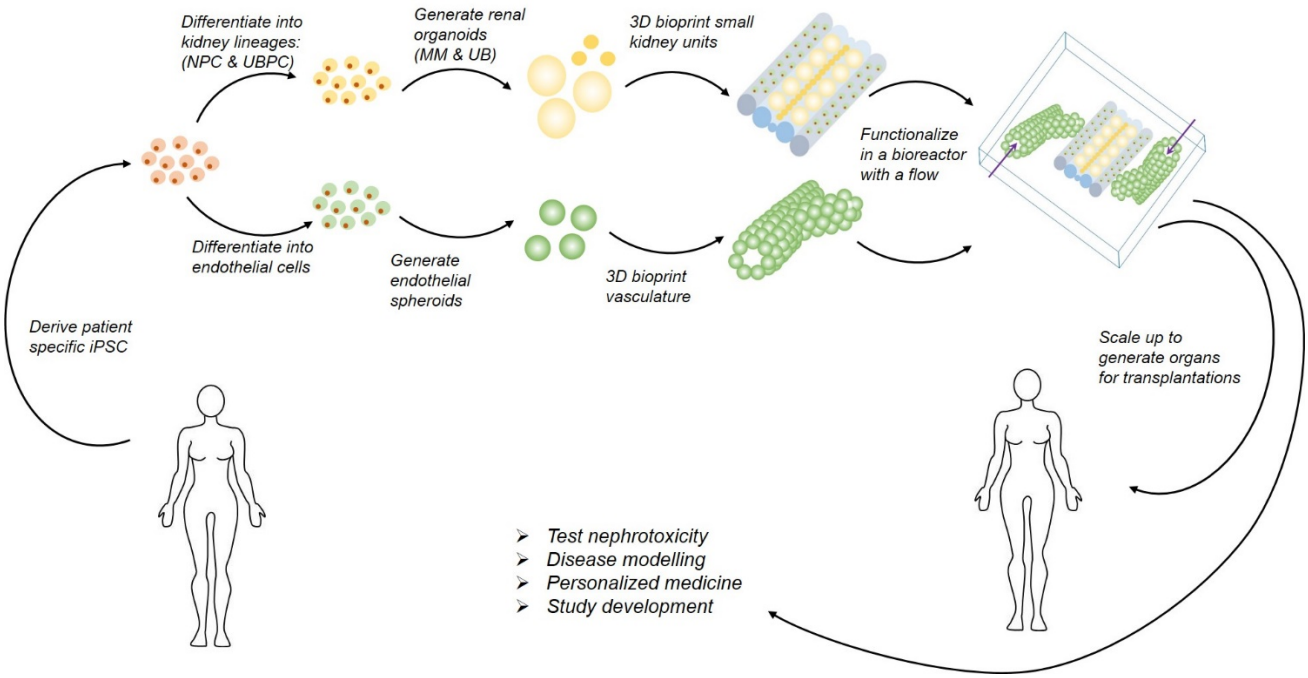


**Figure 3.** Schematic of possible workflow towards successful 3D bioprinting of a kidney. The somatic cells taken as a biopsy from a patient can be used to generate iPSCs (using non-integrating methods) and differentiated into NPCs, UBPCs or endothelial cells using available protocols. These lineage specific cells will then generate spheroids/organoids, which will be used as building blocks to 3D bioprint tissues. The NPCs and UBPCs will generate renal organoids, UBPCs will generate UB spheroids; the organoids will be printed in close proximity to each other allowing fusion in order to generate more compact mass tissue, while the UB spheroids will be printed in the middle to generate a drainage system. The endothelial cells will generate endothelial spheroids, which will be used to 3D bioprint vasculature using different techniques to obtain different diameters, while some single endothelial cells will also be printed in a suitable hydrogel supplemented with VEGF to generate the smallest diameter capillaries upon placement in the microfluidic chamber. The 3D bioprinted vasculature and kidney units could be easily scaled up to generate organs for transplantations. However, even with the small units, it would be beneficial to test the nephrotoxicity of novel or existing drugs, to establish personalized therapies, expand our knowledge about renal development or model various diseases.

### *8.1. Screening platform for nephrotoxicity*

The kidney is very sensitive to the toxic effects of pharmacological compounds, industrial, household and environmental chemicals, food additives and natural substances [172–177]. The renal excretion of toxic substances starts with glomerular filtration of the blood. The primary urine then enters the tubular system, first through the proximal tubule, where the important compounds are re-absorbed, then the loop of Henle, where the filtrate is concentrated. Next, the urine passes in the distal tubule and the collecting duct, where the urine is further concentrated and moved into the bladder for storage until it is finally removed from the body during the micturition process. The

major part of the nephrotoxicity studies focuses on the proximal tubule, where the reabsorption of the toxic compounds causes renal damage.

Due to the limitations in the predictability of the animal models, ~90% of candidate drugs result in failure during human trials [178]. In addition, the available *in vitro* models for studying nephrotoxicity are not fully recapitulating the biological functions of the kidney. In pre-clinical trials, only 7% of new therapeutic agents fail because of their nephrotoxicity but the nephrotoxic effects of the pharmacological compounds are the cause of acute kidney injuries in 17%–26% of the cases in hospitals [179,180]. Even the small units of 3D bioprinted functional kidneys would improve the ability to test the nephrotoxicity of new compounds effectively and efficiently already at the pre-clinical stage. This, on other hand, would enable the earlier termination of faulty drugs or lead to the modification of the therapeutic agent to make it less toxic to the renal cells. This could also diminish the amount of animal experiments needed at the pre-clinical testing stage and could accelerate the research and reduce the costs of developing new pharmaceuticals [181–183].

Various *in vitro* and kidney-on-a-chip models have been developed [184–186], but they all lack the functionality and the *in vivo*-like 3D structure of the real nephron. A kidney-on-a-chip is a microfluidic device that allows the cultivation of renal cells and organoids inside 3D channels, mimicking the physiological environment and recapitulating the renal filtering, absorption and excretion of the drug [187,188]. Typically, they have been comprised of a monolayer of renal cells in a microfluidic chamber, lacking the 3D architecture of the real organ.

The hPSC-derived kidney organoids generated via different protocols by Morizane, Takasato and Freedman were able to respond to nephrotoxicity studies [31–33] but they still lack vasculature and the collecting duct system. The 3D bioprinted and vascularized *in vivo*-like complex of functional kidney would be a more improved renal model. Validation of the model would have to be performed by testing a large number of known nephrotoxic and non-nephrotoxic compounds [189,190]. However, the pharma industry would benefit from a library of hPSC-derived mini-kidneys. These 3D bioprinted kidneys would also serve as personalized testing platforms for nephrotoxicity and for planning personalized treatments to reduce kidney damage and hinder possible kidney failure in patients with already existing risk factors, such as diabetes.

### *8.2. Kidney disease model and personalized medicine*

Chronic kidney disease (CKD) is a group of diseases, some of which are multifactorial in origin and where the molecular basis of the disease is not that well understood. Therefore, renal disease modeling would be another important area where the 3D bioprinted kidney would be of great value. The disease specific kidneys would be generated either through genetically engineered hPSCs, where mutations that cause kidney disease has been introduced [191] or through patient specific hiPSCs. The patient specific kidney disease organoids could then be used for rapid *ex vivo* testing of targeted drug therapy or for genomic repair of the genetic defects. The model would generate data that help us better understand the molecular background and pathophysiology of the disease. It would also be useful as a screening platform for new, targeted treatments [192].

Polycystic kidney disease (PKD) has been modeled using 3D cultures of patient-derived primary cells [193], while Freedman *et al.* have generated iPS cells from PKD patients and showed

reduced levels of polycystin 2 within the cilia of these autosomal dominant polycystic kidney disease (ADPKD) cells and rescued this defect by overexpressing polycystin 1 [194]. The same group also recently published a study on gene-edited PKD kidney organoids [195], in which they introduced a PKD1 mutation to the kidney organoid and studied how cysts form, and identified the modulators of cystogenesis.

In addition, a microfluidic diabetic nephropathy glomerulus-on-a-chip model was recently presented [196] as well as a 3D-co-culture of glomerular endothelial cells, podocytes and mesangial cells [197]; however, these models also lack the *in vivo* 3D structure of the nephron. The latter can be provided by the generation of organoids and has already been proposed to be an excellent platform for disease modeling [198–200].

### *8.3. Studying kidney development*

The kidney is composed of more than 20 different specialized cell types and has the most complex architecture after the central nervous system. The bioprinted and vascularized kidney will have a role in understanding the development of the metanephric kidney and its vascularization. hPSCs/hiPSCs-derived kidney organoids have been recently used to study the differentiation of podocytes and the study underlined the importance of podocalyxin in the generation of podocytes [201].

### *8.4. Regenerative medicine*

The human kidney can regenerate new tubular cells after a case of acute kidney injury, but it lacks the ability to create new nephrons after birth [202]. Therefore, the only options right now to treat chronic kidney failure patients developing ESRD are the dialysis treatment and/or the kidney transplant. With a fast-growing group of people in need of a new kidney, the goal for regenerative medicine in the kidney field is to develop strategies for regenerating and repairing injured areas of the kidney, as well as generate entire kidneys for transplantation. The current organoid model shows an amazing cellular differentiation and tissue architecture potential, but in order to function and secrete urine, the kidney has to be connected to blood circulation and incorporate an excretory system.

The long-term goal of the 3D bioprinted kidneys is to generate transplantable kidney, however the closer and more realistic aim is to establish a minimal functional unit of the kidney, to recapitulate the *in vivo* functional kidney. The question is how simple or how complex should it be?

## 9. Conclusions

The 3D bioprinting technologies are rapidly developing and it will be soon possible to 3D bioprint not only solid tissues but also soft ones, such as the kidney. In fact, many of the technologies are available already. We are able to derive cells from patients and differentiate them efficiently into kidney lineages or endothelial cells, which will provide a wonderful source of cells for generating organoids. We are able to generate well developed renal organoids containing several nephron structures in correct order with functional cells. We can also generate other tissue spheroids, such as those from endothelial cells that may provide source of tissue to 3D bioprint vasculature. All of the

presented advancements could potentially be used as building blocks for 3D bioprinting to print vascularized small kidney units. Both of these components (i.e. the vasculature and the kidney structure) would have to be either printed together or placed together after printing in a microfluidic chamber or a bioreactor, where the applied flow could initiate the capillarization of the developing kidneys (Figure 3).

With regard to the choice of the bioink material for the kidney bioprinting, the kidney-derived decellularized ECM could offer an interesting alternative to achieve improved cell performance if its mechanical integrity is increased by for example mixing it with another hydrogel. Overall, each available bioink type has its inherent pros and cons but by combining two or more complementary bioinks together adequate properties for successful kidney bioprinting could be achieved. Due to the practicality and ability of the EBB technique to fabricate even large tissue constructs, it may well be the printing platform that will enable the fabrication of a larger scale kidney construct. Or perhaps, a totally new bioprinting approach will emerge and overcome the limitations of the current printing modalities.

When considering the needs of regenerative medicine, the 3D bioprinted organs/kidneys can reduce the rate of graft rejection when they are printed using only patient's own cells (hiPSCs). Moreover, a study by Yokoo's Lab presented a new technique, the "stepwise peristaltic ureter" (SWPU) system [203]. The SWPU system enabled the construction of a patent urine excretion system which protected the grafted kidneys from the development of hydronephrosis and permitted continued growth of the transplanted embryonic kidneys. Similar strategy might be used for transplanting 3D bioprinted kidneys.

Therefore, it is just a matter of time, when we will be able, in a correct way, to combine the stem cell expertise with the developmental biology knowledge bringing them together with 3D bioprinting and microfluidic technologies, and consequently put all necessary puzzle pieces together to successfully 3D bioprint the functional units of the kidney.

## Acknowledgements

This work was supported by the Finnish Cultural Foundation (personal research grant #00180086 to S.T. and personal research grant #00160821 to A.R-R), by the Academy of Finland grants (#206038, #121647, #250900 & #260056), and by the Centre of Excellence grant 2012–2017 from the Academy of Finland (#251314).

## Conflict of interest

Authors declare no conflict of interest.

## References

1. European Commision (2014) Journalist Workshop on organ donation and transplantation, Recent facts and figures.

2. Weiner DE (2009) Public health consequences of chronic kidney disease. *Clin Pharmacol Ther* 86: 566–569.
3. Hesuani Y, Pereira FDAS, Parfenov V, et al. (2016) Design and Implementation of Novel Multifunctional 3D Bioprinter. *3D Print Addit Manuf* 3: 64.
4. Colaco M, Igel DA, Atala A (2018) The potential of 3D printing in urological research and patient care. *Nat Rev Urol* 15: 213–221.
5. Cui X, Breitenkamp K, Lotz M, et al. (2012) Synergistic action of fibroblast growth factor-2 and transforming growth factor-beta1 enhances bioprinted human neocartilage formation. *Biotechnol Bioeng* 109: 2357–2368.
6. Murphy SV, Atala A (2014) 3D bioprinting of tissues and organs. *Nat Biotechnol* 32: 773–785.
7. Skardal A, Atala A (2015) Biomaterials for integration with 3-D bioprinting. *Ann Biomed Eng* 43: 730–746.
8. Bulanova EA, Koudan EV, Degosserie J, et al. (2017) Bioprinting of functional vascularized mouse thyroid gland construct. *Biofabrication* 9: 034105.
9. Rak-Raszewska A, Hauser PV, Vainio S (2015) Organ In Vitro Culture: What Have We Learned about Early Kidney Development? *Stem Cells Int* 2015: 959807.
10. Grobstein C (1953) Inductive epitheliomesenchymal interaction in cultured organ rudiments of the mouse. *Sci* 118: 52–55.
11. Grobstein C (1956) Inductive tissue interaction in development. *Adv Cancer Res* 4: 187–236.
12. Saxen L, Wartiovaara J (1966) Cell contact and cell adhesion during tissue organization. *Int J Cancer* 1: 271–290.
13. Herrera M, Mirotsou M (2014) Stem cells: potential and challenges for kidney repair. *Am J Physiol Renal Physiol* 306: F12–23.
14. Auerbach R, Grobstein C (1958) Inductive interaction of embryonic tissues after dissociation and reaggregation. *Exp Cell Res* 15: 384–397.
15. Unbekandt M, Davies JA (2010) Dissociation of embryonic kidneys followed by reaggregation allows the formation of renal tissues. *Kidney Int* 77: 407–416.
16. Junttila S, Saarela U, Halt K, et al. (2015) Functional genetic targeting of embryonic kidney progenitor cells ex vivo. *J Am Soc Nephrol* 26: 1126–1137.
17. Lancaster MA, Knoblich JA (2014) Organogenesis in a dish: modeling development and disease using organoid technologies. *Sci* 345: 1247125.
18. Schutgens F, Verhaar MC, Rookmaaker MB (2016) Pluripotent stem cell-derived kidney organoids: An *in vivo*-like *in vitro* technology. *Eur J Pharmacol* 790: 12–20.
19. Xinaris C, Benedetti V, Rizzo P, et al. (2012) *In vivo* maturation of functional renal organoids formed from embryonic cell suspensions. *J Am Soc Nephrol* 23: 1857–1868.
20. Xinaris C, Benedetti V, Novelli R, et al. (2015) Functional Human Podocytes Generated in Organoids from Amniotic Fluid Stem Cells. *J Am Soc Nephrol* 27: 1400–1411.
21. Bantounas I, Ranjzad P, Tengku F, et al. (2018) Generation of Functioning Nephrons by Implanting Human Pluripotent Stem Cell-Derived Kidney Progenitors. *Stem Cell Reports* 10: 766–779.
22. Bertram JF, Douglas-Denton RN, Diouf B, et al. (2011) Human nephron number: implications for health and disease. *Pediatr Nephrol* 26: 1529–1533.

23. Ogunlade O, Connell JJ, Huang JL, et al. (2017) *In vivo* 3-dimensional photoacoustic imaging of the renal vasculature in preclinical rodent models. *Am J Physiol Renal Physiol* 314: F1145–1153.
24. Wilmer MJ, Saleem MA, Masereeuw R, et al. (2010) Novel conditionally immortalized human proximal tubule cell line expressing functional influx and efflux transporters. *Cell Tissue Res* 339: 449–457.
25. Saleem MA, O'Hare MJ, Reiser J, et al. (2002) A conditionally immortalized human podocyte cell line demonstrating nephrin and podocin expression. *J Am Soc Nephrol* 13: 630–638.
26. Rak-Raszewska A, Wilm B, Edgar D, et al. (2012) Development of embryonic stem cells in recombinant kidneys. *Organog* 8: 125–136.
27. Takasato M, Er PX, Becroft M, et al. (2014) Directing human embryonic stem cell differentiation towards a renal lineage generates a self-organizing kidney. *Nat Cell Biol* 16: 118–126.
28. Taguchi A, Kaku Y, Ohmori T, et al. (2014) Redefining the *in vivo* origin of metanephric nephron progenitors enables generation of complex kidney structures from pluripotent stem cells. *Cell Stem Cell* 14: 53–67.
29. Kang M, Han YM (2014) Differentiation of human pluripotent stem cells into nephron progenitor cells in a serum and feeder free system. *PLoS One* 9: e94888.
30. Toyohara T, Mae S, Sueta S, et al. (2015) Cell Therapy Using Human Induced Pluripotent Stem Cell-Derived Renal Progenitors Ameliorates Acute Kidney Injury in Mice. *Stem Cells Transl Med* 4: 980–992.
31. Takasato M, Er PX, Chiu HS, et al. (2015) Kidney organoids from human iPS cells contain multiple lineages and model human nephrogenesis. *Nat* 526: 564–568.
32. Freedman BS, Brooks CR, Lam AQ, et al. (2015) Modelling kidney disease with CRISPR-mutant kidney organoids derived from human pluripotent epiblast spheroids. *Nat Commun* 6: 8715.
33. Morizane R, Lam AQ, Freedman BS, et al. (2015) Nephron organoids derived from human pluripotent stem cells model kidney development and injury. *Nat Biotechnol* 33: 1193–1200.
34. Morizane R, Bonventre JV (2017) Generation of nephron progenitor cells and kidney organoids from human pluripotent stem cells. *Nat Protoc* 12: 195–207.
35. Xia Y, Sancho-Martinez I, Nivet E, et al. (2014) The generation of kidney organoids by differentiation of human pluripotent cells to ureteric bud progenitor-like cells. *Nat Protoc* 9: 2693–2704.
36. He Y, Yang F, Zhao H, et al. (2016) Research on the printability of hydrogels in 3D bioprinting. *Sci Rep* 6: 29977.
37. Aljohani W, Ullah MW, Zhang X, et al. (2018) Bioprinting and its applications in tissue engineering and regenerative medicine. *Int J Biol Macromol* 107: 261–275.
38. Jose RR, Rodriguez MJ, Dixon TA, et al. (2016) Evolution of Bioinks and Additive Manufacturing Technologies for 3D Bioprinting. *ACS Biomater Sci Eng* 2: 1662–1678.
39. Garreta E, Oria R, Tarantino C, et al. (2017) Tissue engineering by decellularization and 3D bioprinting. *Mater Today* 20: 166–178.
40. Murphy SV, Skardal A, Atala A (2013) Evaluation of hydrogels for bio-printing applications. *J Biomed Mater Res A* 101: 272–284.
41. Cui H, Nowicki M, Fisher JP, et al. (2017) 3D Bioprinting for Organ Regeneration. *Adv Healthc Mater* 6: 1601118.

42. Peppas NA, Bures P, Leobandung W, et al. (2000) Hydrogels in pharmaceutical formulations. *Eur J Pharm Biopharm* 50: 27–46.
43. Drury JL, Mooney DJ (2003) Hydrogels for tissue engineering: scaffold design variables and applications. *Biomater* 24: 4337–4351.
44. Peloso A, Tamburrini R, Edgar L, et al. (2016) Extracellular matrix scaffolds as a platform for kidney regeneration. *Eur J Pharmacol* 790: 21–27.
45. Pati F, Jang J, Ha DH, et al. (2014) Printing three-dimensional tissue analogues with decellularized extracellular matrix bioink. *Nat Commun* 5: 3935.
46. Skardal A, Devarasetty M, Kang HW, et al. (2015) A hydrogel bioink toolkit for mimicking native tissue biochemical and mechanical properties in bioprinted tissue constructs. *Acta Biomater* 25: 24–34.
47. Jang J, Kim TG, Kim BS, et al. (2016) Tailoring mechanical properties of decellularized extracellular matrix bioink by vitamin B2-induced photo-crosslinking. *Acta Biomater* 33: 88–95.
48. Beamish JA, Chen E, Putnam AJ (2017) Engineered extracellular matrices with controlled mechanics modulate renal proximal tubular cell epithelialization. *PLoS One* 12: e0181085.
49. Chen WC, Lin HH, Tang MJ (2014) Regulation of proximal tubular cell differentiation and proliferation in primary culture by matrix stiffness and ECM components. *Am J Physiol Renal Physiol* 307: F695–707.
50. Homan KA, Kolesky DB, Skylar-Scott MA, et al. (2016) Bioprinting of 3D Convoluted Renal Proximal Tubules on Perfusable Chips. *Sci Rep* 6: 34845.
51. Kleinman HK, Martin GR (2005) Matrigel: basement membrane matrix with biological activity. *Semin Cancer Biol* 15: 378–386.
52. Moll S, Ebeling M, Weibel F, et al. (2013) Epithelial cells as active player in fibrosis: findings from an in vitro model. *PLoS One* 8: e56575.
53. Mu X, Zheng W, Xiao L, et al. (2013) Engineering a 3D vascular network in hydrogel for mimicking a nephron. *Lab Chip* 13: 1612–1618.
54. King SM, Higgins JW, Nino CR, et al. (2017) 3D Proximal Tubule Tissues Recapitulate Key Aspects of Renal Physiology to Enable Nephrotoxicity Testing. *Front Physiol* 8: 123.
55. Nguyen DG, King SM, Presnell SC (2016) Engineered Renal Tissues, Arrays Thereof, and Methods of Making the Same.
56. Matak D, Brodaczewska KK, Lipiec M, et al. (2017) Colony, hanging drop, and methylcellulose three dimensional hypoxic growth optimization of renal cell carcinoma cell lines. *Cytotechnology* 69: 565–578.
57. Astashkina AI, Mann BK, Prestwich GD, et al. (2012) A 3-D organoid kidney culture model engineered for high-throughput nephrotoxicity assays. *Biomaterials* 33: 4700–4711.
58. Astashkina AI, Mann BK, Prestwich GD, et al. (2012) Comparing predictive drug nephrotoxicity biomarkers in kidney 3-D primary organoid culture and immortalized cell lines. *Biomaterials* 33: 4712–4721.
59. Ozbolat IT, Hospodiuk M (2016) Current advances and future perspectives in extrusion-based bioprinting. *Biomaterials* 76: 321–343.
60. Alconcel SNS, Baas AS, Maynard HD (2017) FDA-approved poly(ethylene glycol)–protein conjugate drugs. *Polymer Chemistry* 2: 1442–1448.

61. Holzl K, Lin S, Tytgat L, et al. (2016) Bioink properties before, during and after 3D bioprinting. *Biofabrication* 8: 032002.
62. Hospodiuk M, Dey M, Sosnoski D, et al. (2017) The bioink: A comprehensive review on bioprintable materials. *Biotechnol Adv* 35: 217–239.
63. Nguyen KT, West JL (2002) Photopolymerizable hydrogels for tissue engineering applications. *Biomaterials* 23: 4307–4314.
64. Arcaute K, Mann BK, Wicker RB (2006) Stereolithography of three-dimensional bioactive poly(ethylene glycol) constructs with encapsulated cells. *Ann Biomed Eng* 34: 1429–1441.
65. Hockaday LA, Kang KH, Colangelo NW, et al. (2012) Rapid 3D printing of anatomically accurate and mechanically heterogeneous aortic valve hydrogel scaffolds. *Biofabrication* 4: 035005.
66. He Y, Tuck CJ, Prina E, et al. (2017) A new photocrosslinkable polycaprolactone-based ink for three-dimensional inkjet printing. *J Biomed Mater Res B Appl Biomater* 105: 1645–1657.
67. Hribar KC, Soman P, Warner J, et al. (2014) Light-assisted direct-write of 3D functional biomaterials. *Lab Chip* 14: 268–275.
68. Li WW, Li H, Liu ZF, et al. (2009) Determination of residual acrylamide in medical polyacrylamide hydrogel by high performance liquid chromatography tandem mass spectroscopy. *Biomed Environ Sci* 22: 28–31.
69. Rana D, Ramalingam M (2017) Enhanced proliferation of human bone marrow derived mesenchymal stem cells on tough hydrogel substrates. *Mater Sci Eng C Mater Biol Appl* 76: 1057–1065.
70. Hron P, Slechtova J, Smetana K, et al. (1997) Silicone rubber-hydrogel composites as polymeric biomaterials. IX. Composites containing powdery polyacrylamide hydrogel. *Biomaterials* 18: 1069–1073.
71. Xi TF, Fan CX, Feng XM, et al. (2006) Cytotoxicity and altered c-myc gene expression by medical polyacrylamide hydrogel. *J Biomed Mater Res A* 78: 283–290.
72. Xi L, Wang T, Zhao F, et al. (2014) Evaluation of an injectable thermosensitive hydrogel as drug delivery implant for ocular glaucoma surgery. *PLoS One* 9: e100632.
73. Dumortier G, Grossiord JL, Agnely F, et al. (2006) A review of poloxamer 407 pharmaceutical and pharmacological characteristics. *Pharm Res* 23: 2709–2728.
74. Wu W, DeConinck A, Lewis JA (2011) Omnidirectional printing of 3D microvascular networks. *Adv Mater* 23: H178–83.
75. Ozbolat IT (2017) *3D Bioprinting: Fundamentals, principles and Applications*, London: Academy Press.
76. Gómez-Guillén MC, Giménez B, López-Caballero ME, et al. (2011) Functional and bioactive properties of collagen and gelatin from alternative sources: A review. *Food Hydrocolloids* 25: 1813–1827.
77. Kuijpers AJ, van Wachem PB, van Luyn MJ, et al. (2000) *In vivo* compatibility and degradation of crosslinked gelatin gels incorporated in knitted Dacron. *J Biomed Mater Res* 51: 136–145.
78. Kolesky DB, Homan KA, Skylar-Scott MA, et al. (2016) Three-dimensional bioprinting of thick vascularized tissues. *Proc Natl Acad Sci U S A* 113: 3179–3184.
79. McManus MC, Boland ED, Koo HP, et al. (2006) Mechanical properties of electrospun fibrinogen structures. *Acta Biomater* 2: 19–28.

80. Cui X, Boland T (2009) Human microvasculature fabrication using thermal inkjet printing technology. *Biomater* 30: 6221–6227.
81. Fussenegger M, Meinhart J, Hobling W, et al. (2003) Stabilized autologous fibrin-chondrocyte constructs for cartilage repair *in vivo*. *Ann Plast Surg* 51: 493–498.
82. Achilli M, Mantovani D (2010) Tailoring Mechanical Properties of Collagen-Based Scaffolds for Vascular Tissue Engineering: The Effects of pH, Temperature and Ionic Strength on Gelation. *Polymers* 2: 664–680.
83. Park JY, Choi JC, Shim JH, et al. (2014) A comparative study on collagen type I and hyaluronic acid dependent cell behavior for osteochondral tissue bioprinting. *Biofabrication* 6: 035004.
84. Lee KY, Moone DJ (2012) Alginate: Properties and biomedical applications. *Progress in Polymer Science* 37: 106–126.
85. Cohen DL, Lo W, Tsavaris A, et al. (2011) Increased mixing improves hydrogel homogeneity and quality of three-dimensional printed constructs. *Tissue Eng Part C Methods* 17: 239–248.
86. Gudapati H, Dey M, Ozbolat I (2016) A comprehensive review on droplet-based bioprinting: Past, present and future. *Biomaterials* 102: 20–42.
87. Yan J, Huang Y, Chrisey DB (2013) Laser-assisted printing of alginate long tubes and annular constructs. *Biofabrication* 5: 015002.
88. Nguyen DG, Funk J, Robbins JB, et al. (2016) Bioprinted 3D Primary Liver Tissues Allow Assessment of Organ-Level Response to Clinical Drug Induced Toxicity In Vitro. *PLoS One* 11: e0158674.
89. Thirumala S, Gimble JM, Devireddy RV (2013) Methylcellulose based thermally reversible hydrogel system for tissue engineering applications. *Cells* 2: 460–475.
90. Lott JR, McAllister JW, Arvidson SA, et al. (2013) Fibrillar structure of methylcellulose hydrogels. *Biomacromolecules* 14: 2484–2488.
91. Oxlund H, Andreassen TT (1980) The roles of hyaluronic acid, collagen and elastin in the mechanical properties of connective tissues. *J Anat* 131: 611–620.
92. Luo Y, Kirker KR, Prestwich GD (2000) Cross-linked hyaluronic acid hydrogel films: new biomaterials for drug delivery. *J Control Release* 69: 169–184.
93. Jeon O, Song SJ, Lee K, et al. (2007) Mechanical properties and degradation behaviors of hyaluronic acid hydrogels cross-linked at various cross-linking densities. *Carbohydrate Polymers* 70: 251–257.
94. Gruene M, Pflaum M, Hess C, et al. (2011) Laser printing of three-dimensional multicellular arrays for studies of cell-cell and cell-environment interactions. *Tissue Eng Part C Methods* 17: 973–982.
95. Chuah JKC, Zink D (2017) Stem cell-derived kidney cells and organoids: Recent breakthroughs and emerging applications. *Biotechnol Adv* 35: 150–167.
96. Reint G, Rak-Raszewska A, Vainio SJ (2017) Kidney development and perspectives for organ engineering. *Cell Tissue Res* 369: 171–183.
97. Ozbolat I, Khoda A (2014) Design of a New Parametric Path Plan for Additive Manufacturing of Hollow Porous Structures With Functionally Graded Materials. *ASME J Comput Inf Sci Eng* 14: 041005.

98. Kamisuki S, Hagata T, Tezuka C, et al. (1998) A low power, small, electrostatically-driven commercial inkjet head: *Proceedings MEMS 98. IEEE. Eleventh Annual International Workshop on Micro Electro Mechanical Systems. An Investigation of Micro Structures, Sensors, Actuators, Machines and Systems* 1998 Jan 25–29, Heidelberg, Germany, pp. 63–68.
99. Gasperini L, Maniglio D, Motta A, et al. (2015) An electrohydrodynamic bioprinter for alginate hydrogels containing living cells. *Tissue Eng Part C Methods* 21: 123–132.
100. Moghadam H, Samimi M, Samimi A, et al. (2010) Electrospray modeling of highly viscous and non-Newtonian liquids. *Journal of Applied Polymer Science* 118: 1288–1296.
101. Demirci U, Montesano G (2007) Single cell epitaxy by acoustic picolitre droplets. *Lab Chip* 7: 1139–1145.
102. Khalil S, Nam J, Sun W (2005) Multi-nozzle deposition for construction of 3D biopolymer tissue scaffolds. *Rapid Prototyp J* 11: 9–17.
103. Bajaj P, Schweller RM, Khademhosseini A, et al. (2014) 3D biofabrication strategies for tissue engineering and regenerative medicine. *Annu Rev Biomed Eng* 16: 247–276.
104. Bhattacharjee N, Urrios A, Kang S, et al. (2016) The upcoming 3D-printing revolution in microfluidics. *Lab Chip* 16: 1720–1742.
105. Ovsianikov A, Muhleder S, Torgersen J, et al. (2014) Laser photofabrication of cell-containing hydrogel constructs. *Langmuir* 30: 3787–3794.
106. Turunen S, Joki T, Hiltunen ML, et al. (2017) Direct Laser Writing of Tubular Microtowers for 3D Culture of Human Pluripotent Stem Cell-Derived Neuronal Cells. *ACS Appl Mater Interfaces* 9: 25717–25730.
107. Odde DJ, Renn MJ (2000) Laser-guided direct writing of living cells. *Biotechnol Bioeng* 67: 312–318.
108. Delaporte P, Alloncle A (2016) Laser-induced forward transfer: A high resolution additive manufacturing technology. *Optics & Laser Technology* 78: 33–41.
109. Yan Y, Li S, Zhang R, et al. (2009) Rapid prototyping and manufacturing technology: principles, representative techniques, applications and development trends. *Tsinghua Science & Technology* 14: 1–12.
110. Zein I, Hutmacher DW, Tan KC, et al. (2002) Fused deposition modeling of novel scaffold architectures for tissue engineering applications. *Biomaterials* 23: 1169–1185.
111. Boland T, Mironov V, Gutowska A, et al. (2003) Cell and organ printing 2: fusion of cell aggregates in three-dimensional gels. *Anat Rec A Discov Mol Cell Evol Biol* 272: 497–502.
112. Bakhshinejad A, D'Souza R (2015) A brief comparison between available bio-printing methods. *IEEE Great Lakes Biomedical Conference (GLBC)*, 2015 May 14–17, Milwaukee, WI, pp. 1–3.
113. Wilson WC, Boland T (2003) Cell and organ printing 1: protein and cell printers. *Anat Rec A Discov Mol Cell Evol Biol* 272: 491–496.
114. Klebe RJ (1988) Cytoscribing: a method for micropositioning cells and the construction of two- and three-dimensional synthetic tissues. *Exp Cell Res* 179: 362–373.
115. Boland T, Tao X, Damon B, et al. (2007) Drop-on-demand printing of cells and materials for designer tissue constructs. *Mater Sci Eng C* 27: 372–376.
116. Derby B (2008) Bioprinting: Inkjet printing protein and hybrid cell-containing materials and structures. *J Mater Chem* 18: 5717–5721.

117. Choi YJ, Yi HG, Kim SW, et al. (2017) 3D Cell Printed Tissue Analogues: A New Platform for Theranostics. *Theranostics* 7: 3118–3137.
118. Dhariwala B, Hunt E, Boland T (2004) Rapid prototyping of tissue-engineering constructs, using photopolymerizable hydrogels and stereolithography. *Tissue Eng* 10: 1316–1322.
119. Odde DJ, Renn MJ (1999) Laser-guided direct writing for applications in biotechnology. *Trends Biotechnol* 17: 385–389.
120. Ringeisen BR, Kim H, Barron JA, et al. (2004) Laser printing of pluripotent embryonal carcinoma cells. *Tissue Eng* 10: 483–491.
121. Ovsianikov A, Schlie S, Ngezahayo A, et al. (2007) Two-photon polymerization technique for microfabrication of CAD-designed 3D scaffolds from commercially available photosensitive materials. *J Tissue Eng Regen Med* 1: 443–449.
122. Guillemot F, Souquet A, Catros S, et al. (2010) High-throughput laser printing of cells and biomaterials for tissue engineering. *Acta Biomater* 6: 2494–2500.
123. Gittard SD, Narayan RJ (2010) Laser direct writing of micro- and nano-scale medical devices. *Expert Rev Med Devices* 7: 343–356.
124. Jang J, Yi H, Cho D (2016) 3D Printed Tissue Models: Present and Future. *ACS Biomater Sci Eng* 2: 1722–1731.
125. Ozbolat IT, Yu Y (2013) Bioprinting toward organ fabrication: challenges and future trends. *IEEE Trans Biomed Eng* 60: 691–699.
126. Mironov V, Visconti RP, Kasyanov V, et al. (2009) Organ printing: tissue spheroids as building blocks. *Biomaterials* 30: 2164–2174.
127. Jakab K, Norotte C, Marga F, et al. (2010) Tissue engineering by self-assembly and bio-printing of living cells. *Biofabrication* 2: 022001.
128. Chung JHY, Naficy S, Yue Z, et al. (2013) Bio-ink properties and printability for extrusion printing living cells. *Biomater Sci* 1: 763–773.
129. Levato R, Visser J, Planell JA, et al. (2014) Biofabrication of tissue constructs by 3D bioprinting of cell-laden microcarriers. *Biofabrication* 6: 035020.
130. Pati F, Ha DH, Jang J, et al. (2015) Biomimetic 3D tissue printing for soft tissue regeneration. *Biomaterials* 62: 164–175.
131. Kang HW, Lee SJ, Ko IK, et al. (2016) A 3D bioprinting system to produce human-scale tissue constructs with structural integrity. *Nat Biotechnol* 34: 312–319.
132. Rouwkema J, Rivron NC, van Blitterswijk CA (2008) Vascularization in tissue engineering. *Trends Biotechnol* 26: 434–441.
133. Rouwkema J, Khademhosseini A (2016) Vascularization and Angiogenesis in Tissue Engineering: Beyond Creating Static Networks. *Trends Biotechnol* 34: 733–745.
134. Lovett M, Lee K, Edwards A, et al. (2009) Vascularization strategies for tissue engineering. *Tissue Eng Part B Rev* 15: 353–370.
135. Costa-Almeida R, Granja PL, Soares R, et al. (2014) Cellular strategies to promote vascularisation in tissue engineering applications. *Eur Cell Mater* 28: 51–66; discussion 66–67.
136. Novosel EC, Kleinhans C, Kluger PJ (2011) Vascularization is the key challenge in tissue engineering. *Adv Drug Deliv Rev* 63: 300–311.

137. Zhang C, Hou J, Zheng S, et al. (2011) Vascularized atrial tissue patch cardiomyoplasty with omentopexy improves cardiac performance after myocardial infarction. *Ann Thorac Surg* 92: 1435–1442.
138. Hammerman MR (2002) Xenotransplantation of developing kidneys. *Am J Physiol Renal Physiol* 283: F601–606.
139. Halt KJ, Parssinen HE, Junttila SM, et al. (2016) CD146(+) cells are essential for kidney vasculature development. *Kidney Int* 90: 311–324.
140. Robert B, St John PL, Abrahamson DR (1998) Direct visualization of renal vascular morphogenesis in Flk1 heterozygous mutant mice. *Am J Physiol* 275: F164–172.
141. Gao X, Chen X, Taglienti M, et al. (2005) Angioblast-mesenchyme induction of early kidney development is mediated by Wt1 and Vegfa. *Development* 132: 5437–5449.
142. Robert B, St John PL, Hyink DP, et al. (1996) Evidence that embryonic kidney cells expressing flk-1 are intrinsic, vasculogenic angioblasts. *Am J Physiol* 271: F744–753.
143. Hyink DP, Tucker DC, St John PL, et al. (1996) Endogenous origin of glomerular endothelial and mesangial cells in grafts of embryonic kidneys. *Am J Physiol* 270: F886–899.
144. Loughna S, Hardman P, Landels E, et al. (1997) A molecular and genetic analysis of renalglomerular capillary development. *Angiogenesis* 1: 84–101.
145. Rymer CC, Sims-Lucas S (2015) In utero intra-cardiac tomato-lectin injections on mouse embryos to gauge renal blood flow. *J Vis Exp* 2015: 52398 .
146. Serluca FC, Drummond IA, Fishman MC (2002) Endothelial signaling in kidney morphogenesis: a role for hemodynamic forces. *Curr Biol* 12: 492–497.
147. Bersini S, Moretti M (2015) 3D functional and perfusable microvascular networks for organotypic microfluidic models. *J Mater Sci Mater Med* 26: 180.
148. Song JW, Bazou D, Munn LL (2015) Microfluidic model of angiogenic sprouting. *Methods Mol Biol* 1214: 243–254.
149. Jeon JS, Bersini S, Gilardi M, et al. (2015) Human 3D vascularized organotypic microfluidic assays to study breast cancer cell extravasation. *Proc Natl Acad Sci U S A* 112: 214–219.
150. Miller JS, Stevens KR, Yang MT, et al. (2012) Rapid casting of patterned vascular networks for perfusable engineered three-dimensional tissues. *Nat Mater* 11: 768–774.
151. Kolesky DB, Truby RL, Gladman AS, et al. (2014) 3D bioprinting of vascularized, heterogeneous cell-laden tissue constructs. *Adv Mater* 26: 3124–3130.
152. Huling J, Ko IK, Atala A, et al. (2016) Fabrication of biomimetic vascular scaffolds for 3D tissue constructs using vascular corrosion casts. *Acta Biomater* 32: 190–197.
153. Atala A (2004) Tissue engineering for the replacement of organ function in the genitourinary system. *Am J Transplant* 4 Suppl 6: 58–73.
154. Cui T, Terlecki R, Atala A (2014) Tissue engineering in urethral reconstruction. *Arch Esp Urol* 67: 29–34.
155. Atala A (2011) Tissue engineering of human bladder. *Br Med Bull* 97: 81–104.
156. de Kemp V, de Graaf P, Fledderus JO, et al. (2015) Tissue engineering for human urethral reconstruction: systematic review of recent literature. *PLoS One* 10: e0118653.

157. Hirashima T, Hoshuyama M, Adachi T (2017) *In vitro* tubulogenesis of Madin-Darby canine kidney (MDCK) spheroids occurs depending on constituent cell number and scaffold gel concentration. *J Theor Biol* 435: 110–115.
158. Zhang K, Fu Q, Yoo J, et al. (2017) 3D bioprinting of urethra with PCL/PLCL blend and dual autologous cells in fibrin hydrogel: An *in vitro* evaluation of biomimetic mechanical property and cell growth environment. *Acta Biomater* 50: 154–164.
159. Mironov V, Kasyanov V, Drake C, et al. (2008) Organ printing: promises and challenges. *Regen Med* 3: 93–103.
160. Visconti RP, Kasyanov V, Gentile C, et al. (2010) Towards organ printing: engineering an intra-organ branched vascular tree. *Expert Opin Biol Ther* 10: 409–420.
161. Kelm JM, Lorber V, Snedeker JG, et al. (2010) A novel concept for scaffold-free vessel tissue engineering: self-assembly of microtissue building blocks. *J Biotechnol* 148: 46–55.
162. Itoh M, Nakayama K, Noguchi R, et al. (2015) Scaffold-Free Tubular Tissues Created by a Bio-3D Printer Undergo Remodeling and Endothelialization when Implanted in Rat Aortae. *PLoS One* 10: e0136681.
163. Norotte C, Marga FS, Niklason LE, et al. (2009) Scaffold-free vascular tissue engineering using bioprinting. *Biomaterials* 30: 5910–5917.
164. Gentile C, Fleming PA, Mironov V, et al. (2008) VEGF-mediated fusion in the generation of uniluminal vascular spheroids. *Dev Dyn* 237: 2918–2925.
165. Fleming PA, Argraves WS, Gentile C, et al. (2010) Fusion of uniluminal vascular spheroids: a model for assembly of blood vessels. *Dev Dyn* 239: 398–406.
166. Davis GE, Bayless KJ, Mavila A (2002) Molecular basis of endothelial cell morphogenesis in three-dimensional extracellular matrices. *Anat Rec* 268: 252–275.
167. Kamei M, Saunders WB, Bayless KJ, et al. (2006) Endothelial tubes assemble from intracellular vacuoles *in vivo*. *Nature* 442: 453–456.
168. Nunes SS, Krishnan L, Gerard CS, et al. (2010) Angiogenic potential of microvessel fragments is independent of the tissue of origin and can be influenced by the cellular composition of the implants. *Microcirculation* 17: 557–567.
169. Laschke MW, Menger MD (2015) Adipose tissue-derived microvascular fragments: natural vascularization units for regenerative medicine. *Trends Biotechnol* 33: 442–448.
170. Alajati A, Laib AM, Weber H, et al. (2008) Spheroid-based engineering of a human vasculature in mice. *Nat Methods* 5: 439–445.
171. Klein D (2018) iPSCs-based generation of vascular cells: reprogramming approaches and applications. *Cell Mol Life Sci* 75: 1411–1433.
172. Pazhayattil GS, Shirali AC (2014) Drug-induced impairment of renal function. *Int J Nephrol Renovasc Dis* 7: 457–468.
173. Perneger TV, Whelton PK, Klag MJ (1994) Risk of kidney failure associated with the use of acetaminophen, aspirin, and nonsteroidal antiinflammatory drugs. *N Engl J Med* 331: 1675–1679.
174. Kataria A, Trasande L, Trachtman H (2015) The effects of environmental chemicals on renal function. *Nat Rev Nephrol* 11: 610–625.

175. Gutierrez OM (2013) Sodium- and phosphorus-based food additives: persistent but surmountable hurdles in the management of nutrition in chronic kidney disease. *Adv Chronic Kidney Dis* 20: 150–156.
176. Jha V, Rathi M (2008) Natural medicines causing acute kidney injury. *Semin Nephrol* 28: 416–428.
177. Isnard Bagnis C, Deray G, Baumelou A, et al. (2004) Herbs and the kidney. *Am J Kidney Dis* 44: 1–11.
178. Gintant G, Sager PT, Stockbridge N (2016) Evolution of strategies to improve preclinical cardiac safety testing. *Nat Rev Drug Discov* 15: 457–471.
179. Mehta RL, Pascual MT, Soroko S, et al. (2004) Spectrum of acute renal failure in the intensive care unit: the PICARD experience. *Kidney Int* 66: 1613–1621.
180. Uchino S, Kellum JA, Bellomo R, et al. (2005) Acute renal failure in critically ill patients: a multinational, multicenter study. *JAMA* 294: 813–818.
181. Chu X, Bleasby K, Evers R (2013) Species differences in drug transporters and implications for translating preclinical findings to humans. *Expert Opin Drug Metab Toxicol* 9: 237–252.
182. Greek R, Menache A (2013) Systematic reviews of animal models: methodology versus epistemology. *Int J Med Sci* 10: 206–221.
183. Olson H, Betton G, Robinson D, et al. (2000) Concordance of the toxicity of pharmaceuticals in humans and in animals. *Regul Toxicol Pharmacol* 32: 56–67.
184. Huang HC, Chang YJ, Chen WC, et al. (2013) Enhancement of renal epithelial cell functions through microfluidic-based coculture with adipose-derived stem cells. *Tissue Eng Part A* 19: 2024–2034.
185. Jang KJ, Cho HS, Kang DH, et al. (2011) Fluid-shear-stress-induced translocation of aquaporin-2 and reorganization of actin cytoskeleton in renal tubular epithelial cells. *Integr Biol (Camb)* 3: 134–141.
186. Sciancalepore AG, Sallustio F, Girardo S, et al. (2014) A bioartificial renal tubule device embedding human renal stem/progenitor cells. *PLoS One* 9: e87496.
187. Sochol RD, Gupta NR, Bonventre JV (2016) A Role for 3D Printing in Kidney-on-a-Chip Platforms. *Curr Transplant Rep* 3: 82–92.
188. Lee J, Kim S (2018) Kidney-on-a-Chip: a New Technology for Predicting Drug Efficacy, Interactions, and Drug-induced Nephrotoxicity. *Curr Drug Metab* 19: 577–583.
189. Wilmer MJ, Ng CP, Lanz HL, et al. (2016) Kidney-on-a-Chip Technology for Drug-Induced Nephrotoxicity Screening. *Trends Biotechnol* 34: 156–170.
190. Xie HG, Wang SK, Cao CC, et al. (2013) Qualified kidney biomarkers and their potential significance in drug safety evaluation and prediction. *Pharmacol Ther* 137: 100–107.
191. Cruz NM, Freedman BS (2018) CRISPR Gene Editing in the Kidney. *Am J Kidney Dis* 71: 874–883.
192. Mundel P (2017) Podocytes and the quest for precision medicines for kidney diseases. *Pflugers Arch* 469: 1029–1037.
193. Jansson K, Nguyen AN, Magenheimer BS, et al. (2012) Endogenous concentrations of ouabain act as a cofactor to stimulate fluid secretion and cyst growth of in vitro ADPKD models via cAMP and EGFR-Src-MEK pathways. *Am J Physiol Renal Physiol* 303: F982–90.
194. Freedman BS, Lam AQ, Sundsbak JL, et al. (2013) Reduced ciliary polycystin-2 in induced pluripotent stem cells from polycystic kidney disease patients with PKD1 mutations. *J Am Soc Nephrol* 24: 1571–1586.

195. Cruz NM, Song X, Czerniecki SM, et al. (2017) Organoid cystogenesis reveals a critical role of microenvironment in human polycystic kidney disease. *Nat Mater* 16: 1112–1119.
196. Wang L, Tao T, Su W, et al. (2017) A disease model of diabetic nephropathy in a glomerulus-on-a-chip microdevice. *Lab Chip* 17: 1749–1760.
197. Waters JP, Richards YC, Skepper JN, et al. (2017) A 3D tri-culture system reveals that activin receptor-like kinase 5 and connective tissue growth factor drive human glomerulosclerosis. *J Pathol* 243: 390–400.
198. Freedman BS (2015) Modeling Kidney Disease with iPS Cells. *Biomark Insights* 10: 153–169.
199. Clevers H (2016) Modeling Development and Disease with Organoids. *Cell* 165: 1586–1597.
200. Garreta E, Montserrat N, Belmonte JCI (2018) Kidney organoids for disease modeling. *Oncotarget* 9: 12552–12553.
201. Kim YK, Refaeli I, Brooks CR, et al. (2017) Gene-Edited Human Kidney Organoids Reveal Mechanisms of Disease in Podocyte Development. *Stem Cells* 35: 2366–2378.
202. Little MH, McMahon AP (2012) Mammalian kidney development: principles, progress, and projections. *Cold Spring Harb Perspect Biol* 4: a008300.
203. Yokote S, Matsunari H, Iwai S, et al. (2015) Urine excretion strategy for stem cell-generated embryonic kidneys. *Proc Natl Acad Sci U S A* 112: 12980–12985.


AIMS Press